

Note: This work has not yet been peer-reviewed and is provided by the contributing author(s) via Earth-ArXiv.org as a means to ensure timely dissemination of scholarly and technical work on a noncommercial basis. Copyright and all rights therein are maintained by the author(s) or by other copyright owners. It is understood that all persons copying this information will adhere to the terms and constraints invoked by each author's copyright. This work may not be reposted without explicit permission of the copyright owner.

This work has been submitted for review at the *Proceedings of the National Academy of Sciences of the United States of America (PNAS)*. Copyright in this work may be transferred without further notice.

DRAFT

# A multi-control climate policy process for a trusted decision maker

Henri F. Drake<sup>a,b</sup>, Ronald L. Rivest<sup>a,1</sup>, Alan Edelman<sup>a</sup>, and John Deutch<sup>a</sup>

<sup>a</sup>Massachusetts Institute of Technology, 77 Massachusetts Ave, Cambridge, MA 02139, USA; <sup>b</sup>MIT-WHOI Joint Program in Oceanography/Applied Ocean Science & Engineering, Cambridge and Woods Hole, MA, 02139, USA

This manuscript was compiled on May 22, 2020

**Persistent greenhouse gas (GHG) emissions threaten global climate goals (1) and have prompted consideration of climate controls supplementary to emissions mitigation (2, 3). We present an idealized model of optimally-controlled climate change (based on 4), which is complementary to simpler analytical models (5) and more comprehensive Integrated Assessment Models (6). We show that the four methods of controlling climate damage—mitigation, carbon dioxide removal, adaptation, and solar radiation modification—are not interchangeable, as they enter at different stages of the causal chain that connects GHG emissions to climate damages. Early and aggressive mitigation is always necessary to stabilize GHG concentrations at a tolerable level (7). The most cost-effective way of keeping warming below 2°C is a combination of all four controls; omitting solar radiation modification—a particularly contentious climate control (8–10)—increases net control costs by 31%. At low discount rates, near-term mitigation and carbon dioxide removal are used to permanently reduce the warming effect of GHGs. At high discount rates, however, GHGs concentrations increase rapidly and future generations are required to use solar radiation modification to offset a large greenhouse effect. We propose a policy response process wherein climate policy decision-makers re-adjust their policy prescriptions over time based on evolving climate outcomes and revised model assumptions. We demonstrate the utility of the process by applying it to three hypothetical scenarios in which model biases in 1) baseline emissions, 2) geoengineering (CDR and SRM) costs, and 3) climate feedbacks are revealed over time and control policies are re-adjusted accordingly.**

Climate policy | Mitigation | Adaptation | Geoengineering | Integrated Assessment Model

Climate change due to anthropogenic greenhouse gas (GHG) emissions poses an existential threat to society (11). Ever since the direct link between GHGs and global warming was established in climate models over fifty years ago (12), scientists have advocated for substantial emissions mitigation to stabilize global GHG concentrations and temperatures (13). The discovery that humans were unintentionally modifying the climate was unsurprisingly followed by speculation about intentional climate control (14). With every year of increasing GHG emissions and climate goals slipping out of reach (1), calls for serious consideration of climate controls beyond just mitigation—and their implications—grow louder (3, 15–18).

Four climate controls have emerged as plausible candidates for use in the near future: emissions Mitigation, carbon dioxide Removal (CDR), Geo-engineering by Solar Radiation Modification (SRM), and Adaptation. The four controls are not directly interchangeable as they enter at different stages of the

causal chain of climate damages (Figure 1; 4, 5):

$$\text{Emissions} \xrightarrow{M} \text{GHGs} \xrightarrow{R} \text{Forcing} \xrightarrow{G} \text{Warming} \xrightarrow{A} \text{Damages.} \quad [1]$$

Controls further down the chain generally carry greater risks, since they require carefully off-setting the various downstream effects of GHG emissions, but also have advantages: CDR is the only control that decreases GHG concentrations; SRM is quick to deploy and has low direct costs (19); and adaptation allows for flexibility in the other controls as any residual climate damages can be reduced by adapting to the new climate, to some extent (20).

Numerous social or geopolitical factors may substantially limit or block deployments of certain controls: problems related to inequity (21), distrust (22, 23), or lack of governance (24, 25) are just a handful of examples. Here, we ignore many of these complexities—except in as much they are implicitly included in costs and socio-technological constraints—and focus on the "best-case" scenario where a globally-trusted decision-maker prescribes global control policies and their policy prescriptions are exactly realized.

Our hypothetical trusted decision-maker must follow some set of principles on which to base their control policies. Two commonly-studied approaches are 1) the cost-benefit approach (e.g. 26), in which control costs are balanced against the benefits of avoided damages, and 2) the cost-effectiveness approach (e.g. 27), in which control costs are minimized subject to a prescribed climate constraint. The cost-effectiveness approach underlies the Paris Climate Agreement (28), which aims to keep global warming well below 2°C above pre-industrial levels and currently organizes global climate policy\*.

\*Intended nationally determined contributions to this effort imply 2.6–3.1°C of warming and will need to be strengthened at upcoming re-negotiations (and realized) to have a reasonable chance

## Significance Statement

We present a simple framework and readily available open source software for optimizing trade-offs between the four primary methods that control human-caused climate damages: 1) reducing anthropogenic greenhouse-gas emissions, 2) removing carbon dioxide from the atmosphere, 3) reducing incoming sunlight through solar radiation modification, and 4) adapting to a changed climate. We describe a policy response process that permits a decision maker to adjust policies and improve model parameters over time based on climate outcomes and research results.

HFD wrote the paper, ran the simulations, and performed the analysis. All authors contributed to the conception of the project, interpretation of the results, and editing of the paper.

<sup>1</sup>To whom correspondence should be addressed. E-mail: rivest@mit.edu

49 The conventional tool for optimizing global climate control  
 50 are Integrated Assessment Models (IAMs), which are the  
 51 result of coupling simple climate system models to simple  
 52 energy-economy models (see 30, for a general overview of IAMs  
 53 and their utility to date). In this paper, we 1) present an  
 54 idealized model of optimally-controlled climate change which  
 55 is complementary to both simpler analytical models and more  
 56 comprehensive IAMs and 2) we propose a sequential policy  
 57 process for periodic and critical re-evaluation of inevitably  
 58 biased forecasts, which we illustrate with three hypothetical  
 59 examples.

## 60 MARGO: An idealized model of optimally-controlled cli- 61 mate change

62 The MARGO model consists of a physical energy bal-  
 63 ance model of Earth’s climate coupled to an idealized socio-  
 64 economic model of climate damages and controls (Figure 1):

- Mitigation of greenhouse gas emissions,
- Adaptation to climate impacts,
- Removal of carbon dioxide (CDR),
- Geoengineering by solar radiation modification (SRM), and
- Optimal deployment of available controls.

66 The model is modular, fast, and customizable and can be run  
 67 with several options of objective functions and constraints.

68 Each of the climate controls acts, in its own distinct way,  
 69 to reduce the damages caused by a changing climate but carry  
 70 their own deployment costs (including direct costs, research  
 71 and development costs, infrastructure costs, regulatory costs).  
 72 The model is designed to include key features of climate physics,  
 73 economics, and policy as concisely as possible and in ways  
 74 consistent with both theory and more comprehensive General  
 75 Circulation Models and IAMs. The shortcoming of the model’s  
 76 simplicity is that while its results provide qualitative insights,  
 77 the quantitative results are unreliable.

78 The model is developed in open source using the Julia pro-  
 79 gramming language (31) at [github.com/hdrake/OptimizeClimate](https://github.com/hdrake/OptimizeClimate)  
 80 (Drake et al., 2020). The model originated as an extension of  
 81 a previous model (4) to time-dependent control variables, al-  
 82 though many improvements have been made since then. Each  
 83 model component is expressed in closed form to facilitate  
 84 analytical analysis and computation. Unlike most idealized  
 85 climate-economic models, the entire MARGO framework can  
 86 be explicitly written down in one or two expressions (SI Text  
 87 2). A derivation and interpretation of the two-box energy  
 88 balance model– which has the same form as that of DICE  
 89 (32)– is included in the Methods. The parameter values used  
 90 throughout the paper are set to the defaults mentioned in  
 91 this section (and comprehensively listed in SI Text 2), except  
 92 where explicitly stated otherwise. Validation experiments are  
 93 summarized in the Methods and described in detail in the  
 94 Supplemental Information.

95 **No-policy baseline scenario.** Climate-controlled scenarios are  
 96 considered relative to an exogenous no-policy baseline where  
 97 carbon-dioxide equivalent ( $\text{CO}_{2e}$ ) emissions  $q(t)$  increase lin-  
 98 early four-fold by 2100 relative to 2020 and decrease linearly  
 99 to zero by 2150, resulting in  $7.3 \text{ W/m}^2$  of radiative forcing  
 100 by 2100 and  $8.5 \text{ W/m}^2$  by 2150, relative to preindustrial lev-  
 101 els. As a result of this forcing, the global-mean temperature

of keeping warming below  $2^\circ \text{C}$  (29).

reaches  $2^\circ \text{C}$  by 2050 and soars to  $T \approx 4.75^\circ \text{C}$  by 2100, relative  
 to preindustrial. We interpret this emission scenario as an  
 idealized extension of the SSP3 baseline scenario, which is  
 characterized by fossil-fueled growth (33).

There are five steps in the causal chain (eq. 1) between  
 $\text{CO}_{2e}$  emissions and climate damages.

1.  $\text{CO}_{2e}$  is emitted at a rate  $q(t)$ , with only a fraction  
 $r = 50\%$  (34) remaining in the atmosphere after a few  
 years, net of uptake by the ocean and terrestrial biosphere  
 (Figure 2a).
2.  $\text{CO}_{2e}$  concentrations increase as long as the emissions  $q(t)$   
 are non-zero, and are given by  $c(t) = c_0 + \int_{t_0}^t r q(t) dt$   
 (Figure 2b).
3. Increasing  $\text{CO}_{2e}$  concentrations strengthen the greenhouse  
 effect, reducing outgoing longwave radiation and causing  
 an increased radiative forcing of  $F(t) = a \ln(c(t)/c_0)$ ,  
 which exerts a warming effect on the surface.
4. Near-surface air temperatures eventually increase by  
 $T(t) = F(t)/B$  to balance the reduced cooling to space,  
 where  $B/(B + \kappa) = 60\%$  of the warming occurs within a  
 few years and the remaining  $\kappa/(B + \kappa) = 40\%$  occurs over  
 the course of several centuries due to ocean heat uptake  
 (35). The feedback parameter  $B$  includes the effects of all  
 climate feedbacks, except those involving the carbon cycle  
 and the long-term ice sheet response (Figure 2c), and the  
 ocean heat uptake rate  $\kappa$  parameterizes the combined  
 effects of advection and diffusion of heat into the deep  
 ocean.
5. Anthropogenic warming causes a myriad of climate im-  
 pacts, which result in damages that increase non-linearly  
 with temperature,  $D = \beta T^2$ .

**Effects of climate controls.** The four available climate controls  
 enter as fractional controls at each link of the climate change  
 causal chain (eq. 1).

Mitigation reduces emissions by a factor  $M(t) \in [0, 1]$  such  
 that the controlled emissions that remain in the atmosphere  
 are  $r q(t)(1 - M(t))$ , where  $M = 1$  corresponds to complete  
 decarbonization of the economy.

Removal of  $\text{CO}_{2e}$ ,  $R(t) \in [0, 1]$ , in contrast to mitigation,  
 is de-coupled from instantaneous emissions and is expressed  
 as the fraction of 2020 baseline emissions that are removed  
 from the atmosphere in a given year,  $q_0 R(t)$ . A maximal value  
 of  $R = 1$  corresponds to removing  $60 \text{ GtCO}_{2e}/\text{year}$ , which is  
 more than twice a recent upper-bound estimate of the global  
 potential for negative emission technologies (36).

A useful diagnostic quantity is the effective emissions

$$r q(t)(1 - M(t)) - q_0 R(t), \quad [2]$$

which is the annual rate of  $\text{CO}_{2e}$  accumulation in the atmo-  
 sphere (Figure 2a), with contributions from both emissions  
 mitigation and CDR. The change in  $\text{CO}_{2e}$  concentrations is  
 simply the integral of the effective emissions over time (Figure  
 2b),

$$c_{M,R}(t) = c_0 + \int_{t_0}^t r q(t')(1 - M(t')) dt' - q_0 \int_{t_0}^t R(t') dt'. \quad [3]$$

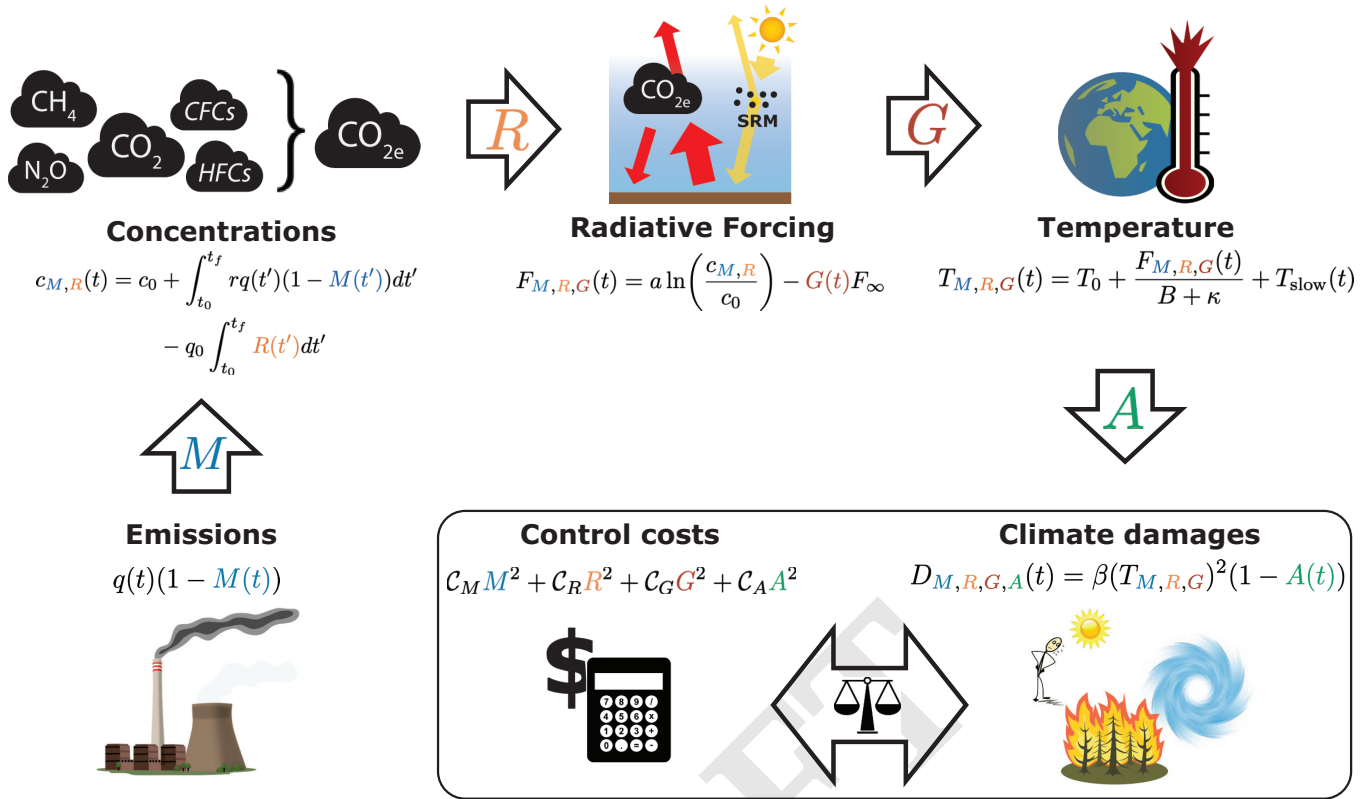


**Fig. 1.** Schematic of the causal chain from greenhouse gas emissions to climate damages, including the unique effects of four climate controls: emissions **Mitigation**, carbon dioxide **Removal**, **Geoengineering** by Solar Radiation Management (SRM), and **Adaptation**. Climate controls yield benefits in terms of avoided climate damages, which are balanced against control deployment costs.

155 **Geoengineering** by SRM,  $G(t) \in [0, 1]$ , acts to offset a  
 156 fraction of the CO<sub>2e</sub> forcing,

$$157 \quad F_{M,R,G}(t) = F_{M,R}(t) - G(t)F_\infty, \quad [4]$$

158 where  $F_{M,R} = a \ln(c_{M,R}(t)/c_0)$  is the controlled CO<sub>2e</sub> forcing  
 159 and  $F_\infty = 8.5 \text{ W/m}^2$  is the maximum baseline CO<sub>2e</sub> forcing,  
 160 which is attained starting in 2150, when baseline emissions are  
 161 assumed to reach zero. A value of  $G = 1$  thus corresponds to a  
 162 complete cancellation between the equilibrium warming from  
 163 baseline CO<sub>2e</sub> increases and the cooling from a full deployment  
 164 of SRM.

165 The controlled near-surface air temperature (Figure 2c)  
 166 evolves according to the total controlled forcing,

$$167 \quad T_{M,R,G}(t) - T_0 = \frac{F_{M,R,G}(t)}{B + \kappa} + \frac{\kappa}{B} \int_{t_0}^t \frac{e^{-\frac{t-t'}{\tau_D}}}{\tau_D} \frac{F_{M,R,G}(t')}{B + \kappa} dt', \quad [5]$$

168 where  $T_0 = 1.1^\circ\text{C}$  is the present warming relative to preindustrial  
 169 and  $\tau_D = 240$  years is the slow timescale of ocean heat  
 170 uptake. The first term on the right-hand side of [5] represents  
 171 a fast transient response while the second term represents a  
 172 slow recalcitrant response due to the thermal inertia of the  
 173 deep ocean (see Methods). Climate inertia decouples the tem-  
 174 perature response from instantaneous forcing and implies that  
 175 an additional fraction of short-term warming (or cooling) is  
 176 locked in for the future, even if radiative forcing is stabilized  
 177 (37), as in the case of bringing emissions to zero in our model<sup>†</sup>.

<sup>†</sup>In earth system models with a dynamic carbon cycle, the slow recalcitrant warming due to a re-

178 **Adaptation** to climate impacts acts to reduce damages by a  
 179 fraction  $A(t) \in [0, 40\%]$ . Since some climate impacts are likely  
 180 impossible to adapt to (20), we assume that adaptation can  
 181 at most reduce climate damages by one-third. The controlled  
 182 damages are thus given by

$$183 \quad D_{M,R,G,A} = \beta(T_{M,R,G})^2(1 - A(t)), \quad [6]$$

184 where the damage parameter  $\beta$  is tuned such that a warm-  
 185 ing of  $3^\circ\text{C}$  results in damages of the 2% of Gross World  
 186 Product (GWP), consistent with DICE in the limit of non-  
 187 catastrophic warming (32). Although adaptation does not  
 188 affect the planetary temperature directly, it is useful to con-  
 189 sider an "adapted temperature"  $T_{M,R,G,A}$  which yields con-  
 190 trolled damages equivalent to the fully-controlled damages  
 191  $\beta(T_{M,R,G,A})^2 = \beta(T_{M,R,G})^2(1 - A)$  and is defined

$$192 \quad T_{M,R,G,A} \equiv T_{M,R,G} \sqrt{1 - A}. \quad [7]$$

193 **Costs and benefits of controlling the climate.** The costs of  
 194 deploying climate controls are non-negligible and must be  
 195 balanced with the benefits of controlling the climate to avoid  
 196 climate impact damages. The costs of climate controls are  
 197 parameterized as:

$$198 \quad C = C_M M^2 + C_R R^2 + C_G G^2 + C_A A^2, \quad [8]$$

199 where the  $C_*$  are the hypothetical annual costs of fully de-  
 200 ploying that control (see Methods) and the cost functions

duction in ocean heat uptake happens to be roughly offset by the ocean carbon sink (34), such that bringing emissions to zero roughly stabilizes temperatures (38). The model's realism would be improved by implementing a simple non-linear model of the ocean carbon cycle (39)

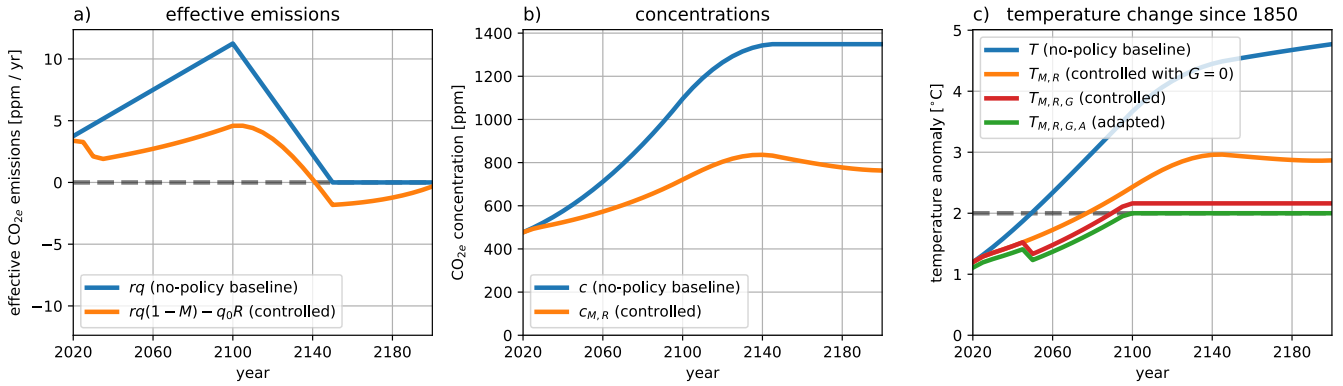


**Fig. 2.** Baseline (blue) and optimally-controlled (orange) a) effective  $\text{CO}_{2e}$  emissions, b)  $\text{CO}_{2e}$  concentrations, and c) temperature anomaly relative to preindustrial from cost-effectiveness analysis. Panel c) shows the optimal temperature change that would occur: in a baseline scenario (blue); with just emissions Mitigation and carbon dioxide Removal (orange); with Mitigation, Removal, and solar-Geoengineering (red); and as an “adapted temperature” (eq. 7) with Adaptation measures also taken into account. The dashed grey line marks the threshold adapted temperature of  $T^* = 2^\circ\text{C}$  to be avoided. In (c),  $T_{M,R,G}$  and  $T_{M,R,G,A}$  decrease slightly in 2050 relative to  $T_{M,R}$  as small but non-zero SRM deployment becomes permissible. Equivalent curves for cost-benefit analysis are shown in Figure S1.

201 are assumed to be convex functions of fractional deployment  
 202 with zero initial marginal cost, as is customary (5, 6, 26), and  
 203 are here all taken to be quadratic for simplicity (4, 5). The  
 204 benefits of deploying climate controls are the avoided climate  
 205 damages relative to the no-policy baseline scenario,

$$206 \quad B = D - D_{M,R,G,A} = \beta(T^2 - (T_{M,R,G,A})^2). \quad [9]$$

207 **Exogenous economic growth.** In contrast to conventional  
 208 IAMs, which follow classic economic theories of optimal eco-  
 209 nomic growth and solve for the maximal welfare based on the  
 210 discounted utility of consumption, we here treat economic  
 211 growth as exogenous (as in 5). The economy, represented by  
 212 the GWP  $E(t) = E_0(1 + \gamma)^{(t-t_0)}$ , grows from its present value  
 213 of  $E_0 = 100$  trillion USD with a fixed growth rate  $\gamma = 2\%$ ,  
 214 consistent with DICE, expert opinion, and an econometric  
 215 forecast model (32, 40). We ignore feedbacks of climate abate-  
 216 ment costs and climate damages on economic growth, since  
 217 they are small variations relative to the exponential rate of  
 218 economic growth in many IAM implementations (32, 41), but  
 219 not all (42).

## 220 Optimal deployments of climate controls

221 A trusted climate policy decision-maker specifies the objective  
 222 function to maximize subject to additional policy constraints.  
 223 The MARGO model is readily optimized in terms of the time-  
 224 dependent climate control variables  $M(t), R(t), G(t), A(t)$ .  
 225 The numerical implementation of the optimization, as well as  
 226 additional socio-technological constraints on the permitted  
 227 timing and rates of deployments, are described in the Meth-  
 228 ods. Here, we describe the optimally-controlled results of two  
 229 policy approaches, cost-benefit analysis and cost-effectiveness  
 230 analysis, and explore their sensitivity to the discount rate  $\rho$   
 231 and possible limits to the fractional penetration of mitigation  
 232  $\mu$ , respectively.

**Cost-benefit analysis.** A natural and widely-used approach is  
 cost-benefit analysis, in which the cost  $C_{M,R,G,A}$  of deploying  
 climate controls is balanced against the benefits  $B_{M,R,G,A}$  of  
 the avoided climate damages. Formally, we aim to maximize

the net present benefits:

$$\max \left\{ \int_{t_0}^{t_f} (B_{M,R,G,A} - C_{M,R,G,A}) (1 + \rho)^{-(t-t_0)} dt \right\}, \quad [10]$$

233 where  $\rho$  is a social discount rate that determines the annual  
 234 depreciation of future costs and benefits of climate control  
 235 to society. There are different views about the appropriate  
 236 non-zero discount rate to apply to multi-generational social  
 237 utility (43–46). Here, we choose a discount rate of  $\rho = 1\%$ , on  
 238 the low end of values used in the literature, motivated by our  
 239 preference towards inter-generational equity (47).

240 The results of maximizing net present benefits are shown in  
 241 Figure 3. Early and aggressive emissions mitigation– and to a  
 242 lesser extent CDR (Fig 3a)– drive net discounted costs of up  
 243 to 1.5 trillion USD/year before 2075 relative to the no-policy  
 244 baseline but deliver orders of magnitude more in net discounted  
 245 benefits from 2075 to 2200 (Fig 3b). Effective  $\text{CO}_{2e}$  emissions  
 246 reach net-zero by 2040 and concentrations stabilize at  $c_{M,R} =$   
 247 500 ppm, slightly above present day  $c_0 = 460$  ppm (Figure  
 248 S1a,b). In 2050, deployments of SRM become permissible and  
 249 quickly scale up to a moderate level of  $G = 15\%$ , permanently  
 250 bringing carbon-controlled temperatures from about  $T_{M,R} \approx$   
 251  $1.5^\circ\text{C}$  to  $T_{M,R,G} \approx 0.75^\circ\text{C}$  above preindustrial (Figure S1c).  
 252 Deployments of adaptation are modest, reflecting its relatively  
 253 high costs and its position at the end of the the causal chain  
 254 of climate damage (eq. 1)

255 The preference for controls earlier in the causal chain, nota-  
 256 bly mitigation, is largely a result of the choice  $\rho = 1\%$  for the  
 257 discount rate (Figure 3c). In particular, if the discount rate in-  
 258 creases above the economic growth rate (48),  $\rho > \gamma = 2\%$ , the  
 259 time decay leads to a different regime of control preferences:  
 260 the short-term fix offered by SRM overwhelmingly becomes the  
 261 preferred control since the high future costs of its unintended  
 262 climate damages are damped by the aggressive discounting of  
 263 future costs. Adaptation emerges as the only control that  
 264 peaks for intermediate values of the discount rate, since its  
 265 benefits are experienced both in the short-term and long-term.

**Cost-effectiveness of avoiding damage thresholds.** The con-  
 266 ventional cost-benefit approach to understanding climate  
 267

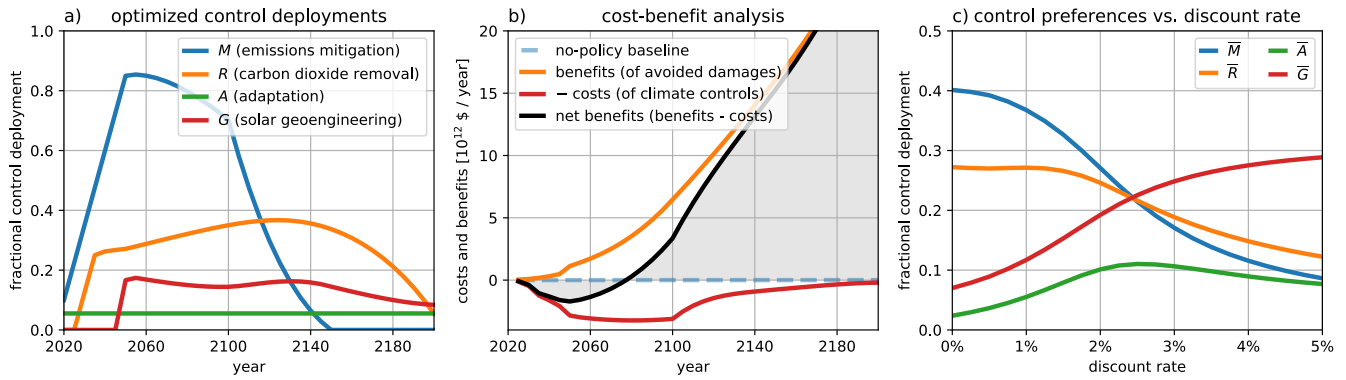


**Fig. 3.** Results of cost-benefit analysis and sensitivity to the discount rate  $\rho$ . (a) Optimal control deployments and (b) corresponding discounted costs and benefits relative to the no climate-policy baseline scenario. The total positive area shaded in grey in (b) is the maximal net present benefits (eq. 10). (c) Time-mean control deployments as a function of the discount rate.

change is limited by the poorly understood damage function (49), which is likely to continue being revised as more is learned about its behavior at high levels of forcing (50, 51). An alternative approach, which presently guides global climate policy negotiations, is to prescribe a threshold of climate damages— or temperatures, as in the Paris Climate Agreement (28)— which is not to be surpassed.

In this implementation, we aim to find the lowest net present costs of control deployments

$$\min \left\{ \int_{t_0}^{t_f} C_{M,R,G,A} (1 + \rho)^{-(t-t_0)} dt \right\} \quad [11]$$

which keep controlled damages below the level corresponding to a chosen temperature threshold,  $\beta(T_{M,R,G})^2(1 - A(t)) < \beta(T^*)^2$ , which we rewrite

$$T_{M,R,G,A} < T^*, \quad [12]$$

where  $T_{M,R,G,A}$  is the "adapted temperature" (eq. 7).

The results of optimizing the cost-effectiveness of controls that keep adapted temperatures below  $T^* = 2^\circ\text{C}$  are shown in Figures 2 and 4. Fractional emissions mitigation increases to a maximum of  $M = 50\%$  decarbonization by 2035 and is maintained until emissions peak in 2100 (Figures 2a and 4a). Carbon dioxide is initially removed at rate of  $Rq_0 \approx 15\% q_0 = 1.1$  ppm/year starting in 2030, which ramps up to  $Rq_0 \approx 30\% q_0 = 2.2$  ppm/year by 2140. Since the optimally-controlled temperatures that result from the above cost-benefit analysis are already lower than  $T^* = 2^\circ\text{C}$ , the optimal controls from cost-effectiveness are less ambitious than for the cost-benefit analysis (Figures 3a, 4a), in contrast to some previous mitigation-only studies (26, 52) but inline with recent analysis (42) that uses an updated climate damage function (51). As a consequence of relatively relaxed mitigation and CDR early on, a sizable deployment of SRM is used to shave off  $1^\circ\text{C}$  degree of warming at its peak in the mid-22nd Century in order to meet the temperature goal (Figure 4a and Figure 2c). Adaptation offsets  $A = 15\%$  of damages and plays a moderate role in reducing damages to below the threshold. Even with discounting, annual costs of control deployments increase until 2100 and remain roughly constant in the 22nd Century (Figure 4b).

To explore the sensitivity of these results to our assumed mitigation costs  $C_M M^2$ , which allow for up to 50% mitigation

by 2035 at the relatively low cost of 700 billion USD/year, we compare the results against a re-optimization with steeper costs at high levels of mitigation. The mitigation cost function is modified to

$$C_M M^2 \left( 1 - e^{-\left(\frac{1-M}{1-\mu}\right)} \right)^{-1}, \quad [13]$$

where we set the penetration limit of cheap mitigation to  $\mu = 40\%$  and the function's structure is shown in Figure 4d. Mitigation costs are unchanged for  $M \ll \mu$ . Around  $M \approx \mu$ , low-hanging mitigation options are increasingly exhausted and costs begin to increase much more rapidly than the default assumption  $M^2$ . The high costs of deep decarbonization drive a reduction in the peak mitigation from  $M = 50\%$  to nearly  $M = 30\%$  in 2060, with the decreased mitigation being compensated by increases in the other three controls (Figure 4c).

### Benefits of a complete portfolio of climate controls

To quantify the benefits of considering a complete portfolio of climate controls, as opposed to considering control technologies in isolation, we compute optimal control trajectories with all 15 combinations of the controls  $\alpha \in \{M, A, R, G\}$ , setting  $\alpha \equiv 0$  for omitted technologies. The most cost-effective strategy includes all four controls and has a net present cost of 136 trillion USD (discount rate of  $\rho = 1\%$ ). Since mitigation is the dominant control in the  $\{MARG\}$  scenario (Figure 4a), the six most cost-effective portfolios include mitigation, with the no-SRM  $\{MAR\}$  and mitigation-plus-CDR  $\{MR\}$  scenarios costing only 31% and 38% more than the  $\{MARG\}$  scenario, respectively (Table 1). The costs in single-control scenarios are much larger, with additional costs of 136% for the mitigation-only scenario  $\{M\}$  to 201% for the SRM-only scenario  $\{G\}$ . In the adaptation-only  $\{A\}$  and CDR-only  $\{R\}$  scenarios, there is no solution that avoids an adapted temperature of  $T^* = 2^\circ\text{C}$ , because we have imposed an adaptability limit  $A < 40\%$  (20) and limits to plausible levels of CDR  $q_0 R < q_0 = 60$  GtCO<sub>2e</sub>/year (see Methods).

### A policy process for responding to uncertain future outcomes

Integrated Assessment Modelling (IAM) approaches assume perfect foreknowledge of model dynamics, parameters (or pa-

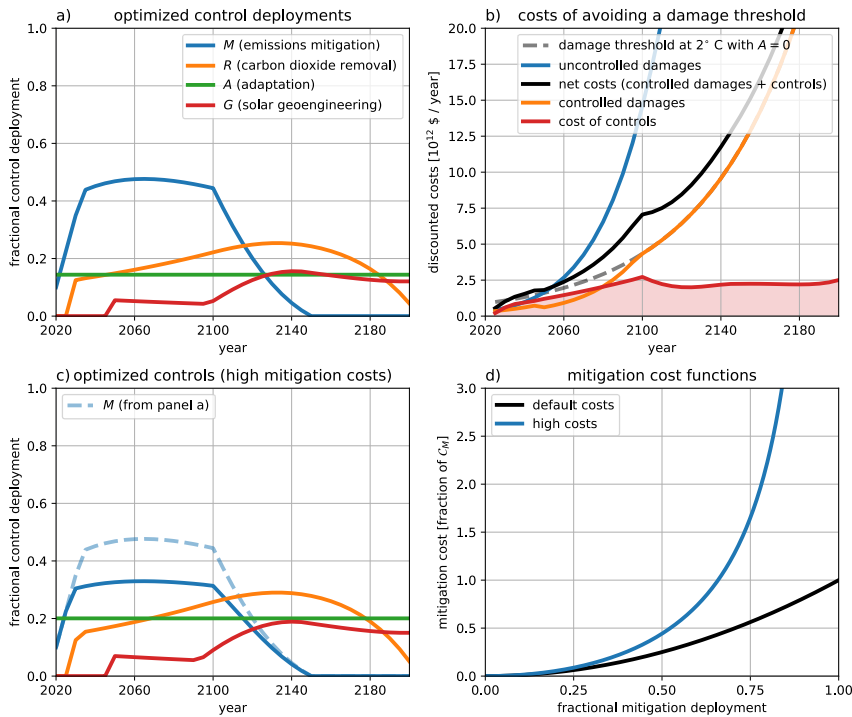


**Fig. 4.** Results of cost-effectiveness analysis and sensitivity to potential limits  $\mu$  to mitigation. (a) Optimal control deployments and (b) corresponding costs and damages. In panel (b), the blue line shows the discounted baseline uncontrolled damages; the dashed grey line shows the discounted damages associated with  $2^\circ$  of warming, which are to be avoided at all costs; the orange line shows the discounted damages in the optimally-controlled solution; and the red line shows the optimal discounted costs of controls such that the shaded area below is the minimal net present costs of controls (eq. 11). (c) Control deployments, as in (a), but re-optimized with high costs of deep decarbonization (blue line in d, eq. 13) relative to the default mitigation costs (black line in d). Mitigation in the default scenario (a) is reproduced as a dashed line in (c) for ease of comparison.

**Table 1.** Additional net present cost of avoiding an adapted temperature of  $T^* = 2^\circ\text{C}$ , relative to the 136 trillion USD net present cost of controls in the  $\{MARG\}$  reference scenario with all four controls available: mitigation (M), adaptation (A), CDR (R) and SRM (G).

MARG	MRG	MAR	MAG	MR	MG	ARG	RG
0%	5%	31%	34%	38%	46%	63%	96%

MA	AG	M	G	AR	R	A
105%	109%	136%	201%	216%	N/A	N/A

Since we have imposed upper bounds  $A < 40\%$  and  $q_0R < q_0 = 60 \text{ GtCO}_2\text{e/year}$  on adaptation and CDR, there is no scenario in which they can, in isolation, keep damages below those associated with  $T^* = 2^\circ\text{C}$  of warming.

model structure and parameter values to correct for revealed biases.

The responsive control strategy process we propose is as follows:

1. Initial future trajectories of optimal control deployments are computed from the vantage point of  $t = t_0$ ;
2. Model projections and control deployments are integrated forward one policy-making period to  $t_1 = t_0 + \Delta t$ ;
3. Model structure and parameter values are revised, owing to new information obtained from observed outcomes and research developments;
4. Future trajectories of control deployments are re-optimized, now from the vantage point of  $t_1 = t_0 + \Delta t$  and with revised model parameters;
5. Return to step 2, replacing  $t_1 = t_0 + \Delta t$  with  $t_n = t_{n-1} + \Delta t$  for period  $n$ , and repeat the process for the desired number of periods.

To illustrate the utility of the policy response process, we apply it to three hypothetical future scenarios, in which the most cost-effective controls for keeping adapted temperatures below  $T^* = 2^\circ\text{C}$  are sequentially re-optimized in response to changes in model inputs and parameters. As a point of reference, we note that the passage of time itself leads to minor adjustments in the optimal combination of control deployments. As each successive generation is exposed to increasingly damaging temperatures, their most cost-effective solution is to increase adaptation measures, which past generations did not yet need, and save costs by slightly decreasing all other controls in the near future (Figure 5a,b). The control adjustments in the three scenarios below (Figure 5c-h) are shown relative to those in the reference case (Figure 5a,b).

parameter distributions), and inputs. Future outcomes will differ from projections because the models are imperfect approximations of the socio-economic and physical climate systems they represent. For example, socio-economic models may assume erroneous future costs of climate controls (53) and physical climate models may omit tipping elements (11), both of which would lead to biases in model projections with respect to actual outcomes. Furthermore, the assumption of perfect foreknowledge degrades the active roles of policy decision-makers in determining baselines and control cost functions, and of climate researchers in refining estimates of physical model parameters.

A hypothetical trusted climate policy decision-maker must be in a position to respond to the inevitable differences that arise between model projections and actual outcomes and to revise their system understanding based on the newest developments in research. We show how our model equips climate policy decision-makers with the ability to periodically re-evaluate policy prescriptions by revising the underlying

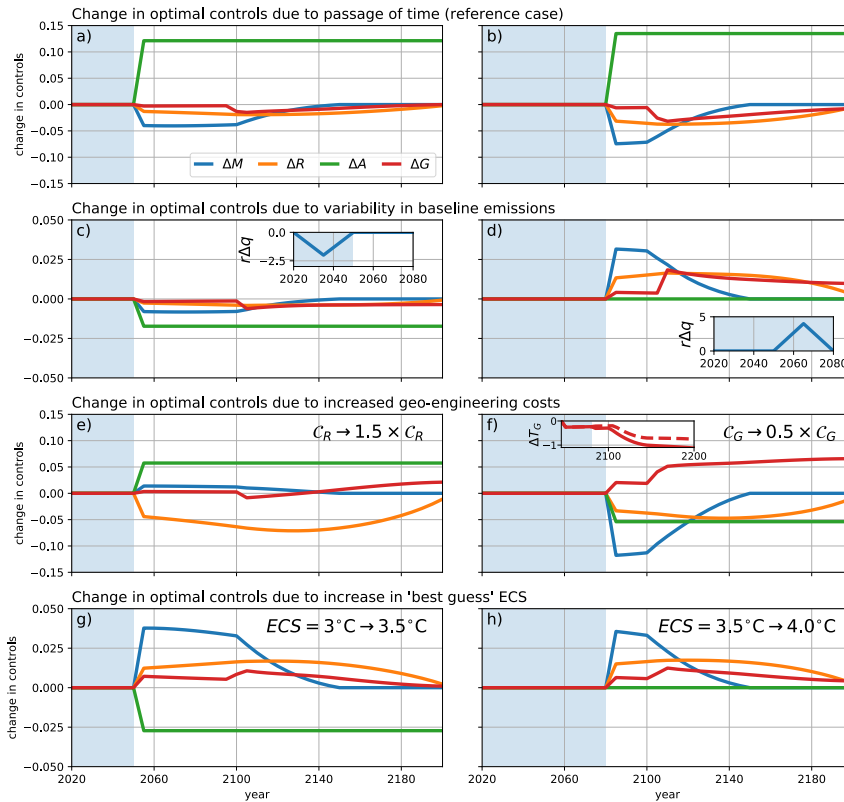


**Fig. 5.** Illustration of the proposed policy process in which the optimally cost-effective control policies are periodically re-adjusted, relative to the original policies prescribed in 2020 (Figure 4a). In a reference case (a,b), time advances sequentially to 2050 (a) and 2080 (b) and policies are re-adjusted to reflect the new timelines. The blue shading shows the passage of time. The changes in control deployments shown in (c-h) are due to sequential re-optimization at 2050 (left) and 2080 (right), relative to the reference case (a,b), but now with revised model parameters: (c,d) where historical effective emissions  $r\Delta q(t)$  are sequentially decreased and then increased (see insets); (e,f) where the costs of CDR and SRM are sequentially increased and decreased, respectively; and (g,h) where the best guess of the Equilibrium Climate Sensitivity (ECS) is revised upwards in 2050 and again in 2080. The inset in (d) shows the cooling due to SRM  $\Delta T_G = T_{M,R,G} - T_{M,R}$  in the default scenario (dashed) and after the re-evaluation in 2080 shown in panel (d) (solid).

**Scenario 1: revealed bias in projected near-term baseline emissions.** Suppose in  $t_0 = 2020$  that the policy decision-maker prescribes aggressive climate control policies based on their cost-effectiveness at keeping warming below  $T^* = 2^\circ\text{C}$  (step 1; Figure 4a) and that these optimal climate controls are perfectly implemented over the following  $\Delta t = 30$  years (step 2).

The policy decision-maker directs a re-evaluation of the optimal control strategy at  $t_1 = 2050$ . The actual baseline emission trajectory between  $t_0 = 2020$  and  $t_1 = 2050$  is found to be  $r\Delta q = 1$  ppm/year lower than projected on average (Figure 5c, inset), resulting in lower  $\text{CO}_{2e}$  concentrations than anticipated and a projected maximum warming of  $\max(T_{M,R,G,A}) = 1.9^\circ\text{C}$ , well below the  $T^* = 2^\circ\text{C}$  goal. The model inputs are thus revised to account for these lower-than-expected historical baseline emissions (step 3) and the optimal future control trajectories are re-computed (step 4). Reduced historical emissions imply a larger remaining carbon budget (54) and allow the policy decision-maker to slightly relax control deployments while still remaining below  $T^* = 2^\circ\text{C}$  of warming (Figure 5c), resulting in 12 trillion USD of avoided net present control costs. At this point, the policy decision maker must decide whether to continue existing policies that lead to  $1.9^\circ\text{C}$  of warming or to reduce future controls deployments (and costs) at the risk of increased climate impacts due to an additional  $0.1^\circ\text{C}$  of warming.

Suppose that, after following the re-optimized control trajectories for another  $\Delta t = 30$  years (step 5), the historical effective baseline emissions must now be revised upwards by 2 ppm/year on average (Figure 5d, inset). With existing policies, the increased historical emissions would result in a  $0.13^\circ\text{C}$  overshoot of the  $T^* = 2^\circ\text{C}$  degree goal. The most cost-effective

adjustment to existing control policies that is consistent with the temperature goal is to increase mitigation, CDR, and SRM efforts by an additional  $\Delta M = 3\%$ ,  $\Delta R = 2\%$ , and  $\Delta G = 2\%$  (Figure 5d), at a net-present cost of 10 trillion USD.

**Scenario 2: revealed bias in projected geoengineering (CDR and SRM) costs.** Suppose that at a re-evaluation in 2050, CDR is found to be 50% more expensive than projected. The climate policy-maker directs deployment of the most cost-effective control trajectories which keep warming below  $T^* = 2^\circ\text{C}$ , which are re-optimized with the revised cost of CDR. The result is to decrease CDR by  $\Delta R = -5\%$  and instead increase adaptation by  $\Delta A = 5\%$  (Figure 5e). The shift away from expensive CDR towards adaptation results in 11.5 trillion USD of avoided net present costs of control deployments, with little difference in climate damage outcomes.

Suppose that after an additional 30 years, during which SRM is ramped up to a modest but non-zero level  $G = 5\%$  (Figure 4a), it becomes clear that the costs of unintended side-effect damages of SRM are less than half as large as expected. In this scenario, the optimal future trajectory is to expand SRM deployments in the 22nd Century to  $G \approx 20\%$  (resulting in  $\Delta T_G = T_{M,R,G} - T_{M,R} \approx -1.0^\circ\text{C}$  of cooling, up from  $-0.6^\circ\text{C}$ ; Figure 5f, inset) and reduce future mitigation levels by  $\Delta M = -10\%$  (Figure 5f), resulting in another 12.6 trillion USD of avoided net present control costs.

**Scenario 3: revealed bias in estimates of climate sensitivity.** Suppose that by 2050, a dramatically improved suite of general circulation climate models robustly exhibits Equilibrium Climate Sensitivities of  $ECS = 3.5^\circ\text{C}$ , up from  $3^\circ\text{C}$  in recent years (55), and further improvements result in  $ECS = 4^\circ\text{C}$

458 by 2080. Each of these revisions effectively shrinks the remain- 518  
459 ing cumulative carbon budget and thus requires sequentially 519  
460 increased deployments of mitigation, CDR, and SRM in order 520  
461 to keep warming below  $T^* = 2^\circ\text{C}$  (Figures 5g, h). 521

462 This responsive policy process only works if adjustments 522  
463 are made sufficiently frequently. If the policy decision-maker 523  
464 had waited from 2020 until 2100 before re-adjusting their 524  
465 course for a higher climate sensitivity of  $ECS = 4^\circ\text{C}$ , there 525  
466 would already be enough warming baked into the system that 526  
467  $T_{M,R,G,A} = 2.2^\circ\text{C} > T^*$  of warming would be inevitable— 527  
468 even if the optimal policy from 2020 (Figure 4a,b) had been 528  
469 perfectly implemented. 529

## 470 Discussion 530

471 Few studies have considered the combined use of mitigation, 531  
472 carbon dioxide removal (CDR), solar radiation modification 532  
473 (SRM), and adaptation for controlling climate damages. We 533  
474 have developed a multi-control, time-dependent model of opti- 534  
475 mally cost-beneficial or cost-effective climate policies, which 535  
476 extends and improves upon previous work (4). Another recent 536  
477 study (5) uses a similar conceptual model with time-dependent 537  
478 controls to analytically investigate the differences between dif- 538  
479 ferent climate controls; however, this model's climate physics 539  
480 are reduced to a simple empirical relationship that is not as 540  
481 clearly applicable to the case of significant SRM, where the 541  
482 direct link between cumulative emissions and temperature 542  
483 falls apart. Despite these differences, our study reproduces 543  
484 two key conceptual results of both earlier studies: 1) the four 544  
485 different climate controls are not interchangeable, as they enter 545  
486 at different stages of the causal chain between emissions and 546  
487 damages, and 2) the most cost-effective solution to limiting 547  
488 climate damages is to use all four controls at our disposal. 548  
489 The first result emerges from the role of each control in modi- 549  
490 fying the basic stock-flow properties of the carbon and heat 550  
491 budgets in the climate system. The second result is a direct 551  
492 consequence of marginal control costs which 1) begin at zero 552  
493 and 2) are concave, and is not guaranteed to hold if either 553  
494 assumption fails. For example, if learning effects are strong 554  
495 enough to cause fractional deployments costs to become con- 555  
496 vex, then a single-control strategy could be more appealing. 556  
497 Alternatively, if substantial R&D investments are necessary 557  
498 before a control is deployed, the large up-front marginal cost 558  
499 may be disqualifying. 559

500 We have proposed a policy response process which high- 560  
501 lights the iterative nature of climate policy decision-making. 561  
502 We show that this process can be used to periodically cor- 562  
503 rect for revealed biases in our understanding of the climate- 563  
504 economic system, in order to avoid unanticipated climate 564  
505 damages or "excessive" spending on climate controls. We view 565  
506 our proposed policy response process as an improvement over 566  
507 previously proposed "sequential" and "adaptive" strategies, in 567  
508 which policies are periodically re-evaluated by following in- 568  
509 structions from a subjectively-defined decision flow chart (e.g. 569  
510 56). In our process, policy re-evaluations are always optimally 570  
511 cost-beneficial or cost-effective, although the parameters that 571  
512 govern this optimization can be periodically re-adjusted. We 572  
513 argue that our policy process based on re-optimization is more 573  
514 defensible than previous approaches but retains the benefits 574  
515 of the process being "adaptive". 575

516 For clarity of exposition, we have presented a fully de- 576  
517 terministic version of the MARGO model. In actuality, key 577  
578

inputs such as the climate feedback parameter  $B$  (and the 518  
related climate sensitivity  $ECS$ ) and the damage function 519  
 $D(T)$  are extremely uncertain. Propagation of these uncer- 520  
tainties through a convex damage function typically increases 521  
expected climate damages and strengthens the case for early 522  
and aggressive climate control (57). Future work includes 1) 523  
extending MARGO to a stochastic programming approach 524  
that accounts for uncertainty in the various input parameters 525  
(see Methods) and 2) implementing a Bayesian policy response 526  
process where prior parameter distributions can be updated 527  
based on observed outcomes (58) or improved parameter esti- 528  
mates from research developments. Stochastic programming 529  
of IAMs is significantly complicated by their endogenous eco- 530  
nomic models (59); the model presented here is significantly 531  
more endogenous and may prove to be a useful framework for 532  
straight-forward multi-stage stochastic programming (60). 533

534 The greatest caveat of the present study may be the assump- 535  
536 tion of a single trusted decision-maker. This device evidently 536  
537 avoids the complexities of a realistic decision making process 537  
538 that involve multiple stake holders with conflicting interests. 538  
539 The costs and benefits defined here are globally-aggregated; 539  
540 asymmetric costs and benefits between different regions lead 540  
541 to diverging incentives, which are further complicated as the 541  
542 number of unique climate controls increases. Asymmetric 542  
543 multi-control incentives can be counter-intuitive: for example, 543  
544 one study suggests that high asymmetry in SRM damages 544  
545 drives even higher levels of mitigation because of the risk of 545  
546 SRM "free-drivers" (61). 546

547 Even in the case where climate control policies are pre- 547  
548 scribed by a single hypothetical decision-maker, there are sure 548  
549 to be inefficiencies in their implementation which we argue 549  
550 are more likely to result in under-deployment of controls than 550  
551 over-deployment. Considerable caution must be taken when- 551  
552 ever relying on substantial CDR or SRM since neither of these 552  
553 controls exist as socio-technological systems capable of influ- 553  
554 encing climate, resulting in a "moral hazard" that shifts the 554  
555 burden to unconsenting future generations (25, 62). 555

556 The MARGO model is an idealized model which highlights 556  
557 the qualitatively different roles of mitigation, CDR, adapta- 557  
558 tion, and SRM in climate control. Both economic and physical 558  
559 components of the model have been abstracted as much as pos- 559  
560 sible to highlight a small number ( $N \approx 9$ ) of key parameters 560  
561 that govern the leading order behavior of the system (as com- 561  
562 pared to widely-used IAMs: 26, 63, 64): the climate feedback 562  
563 parameter  $B$  (related to the equilibrium climate sensitivity 563  
564  $ECS = F_{2\times\text{CO}_2}$ ), the ocean heat uptake rate  $\kappa$ , the exogenous 564  
565 economic growth rate  $\gamma$ , the discount rate  $\rho$ , the climate dam- 565  
566 age parameter  $\beta$ , and the controls costs  $C_M, C_R, C_A, C_G$  (SI 566  
567 Text 2 and Table S1). We show how the model can be used to 567  
568 investigate the sensitivity of "optimal" climate control policies 568  
569 to poorly constrained parameters, such as future control costs, 569  
570 and value-dependent parameters, such as the discount rate. 570  
571 We believe that our model resides in a sweet spot of being more 571  
572 realistic than semi-analytic models and easier to understand 572  
573 than conventional IAMs. We demonstrate that our model can 573  
574 be easily modified to reproduce the qualitative results of other 574  
575 studies (e.g. 6, 65, SI Text 3) and hope that it will be a useful 575  
576 community tool for extending simpler models, interpreting 576  
577 more comprehensive models, and bridging the gaps between 577  
578 climate economists, scientists, policy decision-makers, and the 578  
579 public (66–68). 579

## 579 Materials and Methods

580 All data and figures used in the study can be found at [github.com/hdrake/OptimizeClimate](https://github.com/hdrake/OptimizeClimate) and are readily reproduced or modified by  
581 the Jupyter notebooks therein.  
582

583 **Control costs.** The scaling costs for the four controls used in the  
584 present study are subjectively tuned; we here describe our rationale  
585 for choosing the parameter values. We remind the reader that the  
586 purpose of the MARGO model is to reveal insights about trade  
587 offs between the multiple controls and the dependence of model  
588 results on structural and parameteric choices. The interested reader  
589 can choose their own parameter values and see how the results  
590 change by visiting our web-browser application at [github.com/hdrake/OptimizeClimate](https://github.com/hdrake/OptimizeClimate) (placeholder until we have a better webapp).  
591

592 The costs of mitigation are set according to the Working Group  
593 III contribution to Intergovernmental Panel on Climate Change's  
594 Fifth Assessment Report (69). In aggressive mitigation scenarios  
595 where CO<sub>2e</sub> emissions decrease 78% to 118% by 2100, they estimate  
596 abatement costs of about 2% of GWP (see their Figure 6.21, panel f).  
597 Thus, we set the scaling cost of mitigation controls to  $C_M = \bar{C}_M E(t)$ ,  
598 where the cost of mitigating all emissions is  $\bar{C}_M = 2\%$  of the GWP  
599  $E(t)$ .

600 The costs of CDR are set according to bottom-up cost estimates  
601 from (36, their Table 2). We compute the mean cost of negative-  
602 emissions technologies, where we weight the median cost of each  
603 negative-emissions technology (in USD/tCO<sub>2</sub>) by its upper-bound  
604 potential for carbon-dioxide removal (in GtCO<sub>2</sub>/year). This leads  
605 to a total potential of roughly  $q_0/2 \approx 26$  GtCO<sub>2</sub>/year at an average  
606 cost of  $\bar{C}_R = 110$  USD/tCO<sub>2</sub>. The scaling cost is thus set based  
607 on an estimate for  $R = 50\%$ , i.e.  $C_R \left(\frac{1}{2}\right)^2 = \bar{C}_R q_0/2$  or  $C_R =$   
608  $2\bar{C}_R q_0 = 13$  trillion USD/year.

609 The costs of SRM largely reflect the costs of unintended climate  
610 damages that result due to their imperfect compensation for GHG  
611 forcing (70). Relative to both the costs of unintended damages  
612 and the costs of other climate controls, the direct costs of SRM  
613 measures are thought to be small (19), as in the most commonly  
614 studied proposal of releasing gaseous sulfate aerosol precursors into  
615 the stratosphere to reflect sunlight back to space. The reference cost  
616 of SRM is thus given by  $C_G(t) = \bar{C}_G E(t)$ , where  $\bar{C}_G$  is the damage  
617 due to deploying  $-F_\infty \equiv -F(t \rightarrow \infty) = -8.5 \text{ Wm}^{-2}$  worth of SRM,  
618 as a fraction of the exogenous GWP  $E(t)$ . In the face of considerable  
619 uncertainties about the climate impacts of large-scale SRM (70), we  
620 make the conservative assumption that the unintended damages of  
621 SRM are as large as the uncontrolled damages due to an equivalent  
622 amount of CO<sub>2e</sub> forcing (as in 6, 71), i.e.  $\bar{C}_G \equiv \beta(F_\infty/B)^2 \approx 4.6\%$ ,  
623 where  $F_\infty/B$  is the equilibrium temperature response to a fixed  
624 radiative forcing of  $F_\infty = 8.5 \text{ Wm}^{-2}$ .

625 The costs of adaptation are estimated based on a recent joint  
626 report from the United Nations, the Bill and Melinda Gates Founda-  
627 tion, and the World Bank. They estimate that adaptation measures  
628 costing 1.8 trillion USD from 2020 to 2030 generate more than  
629 five times as much in total net benefits. Here, we make the crude  
630 assumption that this level of spending (180 billion USD / year)  
631 reduces climate damages by  $A = 20\%$ , i.e.  $C_A \left(\frac{1}{5}\right)^2 = 180$  billion  
632 USD / year, or  $C_A = 4.5$  trillion USD / year. We additionally cap  
633 adaptation at  $A < 1/2$ , recognizing that adaptation to all climate  
634 impacts is impossible: there will always be residual damages that  
635 cannot be adapted to (20).

636 **Optimization method.** We use the Interior Point Optimizer (72)  
637 (<https://github.com/coin-or/Ipopt>), an open source software package for  
638 large-scale nonlinear optimization, to minimize objective functions  
639 representing benefits and costs to society subject to assumed policy  
640 constraints. In practice, the control variables  $\alpha \in A = \{M, R, G, A\}$   
641 are discretized into  $N = (t_f - t_0)/\delta t$  timesteps (default  $\delta t = 5$  years,  
642  $N = 36$ ) resulting in a  $4N$ -dimensional optimization problem. In the  
643 default (deterministic and convex) configuration, the model takes  
644 only  $\mathcal{O}(10 \text{ ms})$  to solve after just-in-time compiling and effectively  
645 provides user feedback in real time. This makes the model amenable  
646 to our forthcoming interactive web application, which is inspired by  
647 the impactful En-ROADS model web application (73).

648 The model was designed from the beginning with the goal of  
649 eventual use in stochastic simulations where 1) the deterministic

650 scalar objective function can be generalized to an expected value of  
651 a probabilistic ensemble of simulations that sample an uncertain  
652 parameter space, and 2) deterministic constraints can be generalized  
653 to probabilistic constraints (e.g. having a two-thirds chance of  
654 keeping temperatures below a goal  $T^*$ ), although these features are  
655 still under active development.

656 **Social, technological, and economic inertia.** For each control  $\alpha \in$   
657  $A = \{M, R, G, A\}$ , we assert a maximum deployment rate

$$\left| \frac{d\alpha}{dt} \right| \leq \dot{\alpha}, \quad [14] \quad 658$$

659 as a crude parameterization of social, technological, and economic  
660 inertia (74), which acts to forbid implausibly aggressive deployment  
661 (75) and phase-out scenarios (see SI Text 2 for more discussion).  
662 We set  $\dot{M} \equiv \dot{R} \equiv 1/40 \text{ years}^{-1}$  in line with the most ambitious  
663 climate goals (2) and  $\dot{G} = 1/20 \text{ years}^{-1}$  to reflect the technological  
664 simplicity of attaining a large SRM forcing relative to mitigation  
665 and CDR. We interpret adaptation deployment costs as buying  
666 insurance against future damages at a fixed annual rate  $C_A A^2$ , with  
667  $\dot{A} = 0$ , which can be increased or decreased upon re-evaluation at a  
668 later date.

669 We also set a control readiness condition which optionally limits  
670 how soon each control is "ready" to be deployed. In particular, in  
671 the default configuration we set  $t_R = 2030$  and  $t_G = 2050$  because  
672 CDR has not yet been deployed at a climatically significant scale  
673 (76) and SRM does not yet exist as a socio-technological system  
674 (25).

675 **Two-box energy balance model.** The evolution of the global-mean  
676 near-surface temperature anomaly (relative to the initial time  $t_0 =$   
677 2020) is determined by the two-box linear energy balance model  
678 (77):

$$C_U \frac{dT}{dt} = -BT - \kappa(T - T_D) + F(t), \quad [15] \quad 679$$

$$C_D \frac{dT_D}{dt} = \kappa(T - T_D), \quad [16] \quad 680$$

681 where eq. 15 represents the upper ocean with average temperature  
682 anomaly  $T$ , and eq. 16 represents the deep ocean with an average  
683 temperature  $T_D$ . The near-surface atmosphere exchanges heat  
684 rapidly with the upper ocean and thus the global-mean near-surface  
685 air temperature is also given by  $T$ . The physical model parameters  
686 are: the upper ocean heat capacity  $C_U = 7.3 \text{ W yr m}^{-2} \text{ K}^{-1}$  (in-  
687 cluding a negligible contribution  $C_A \ll C_U$  from the atmosphere);  
688 the deep ocean heat capacity  $C_D = 106 \text{ W yr m}^{-2} \text{ K}^{-1}$ ; the climate  
689 feedback parameter  $B = 1.13 \text{ W m}^{-2} \text{ K}^{-1}$ ; and the ocean mixing  
690 rate  $\kappa = 0.73 \text{ W m}^{-2} \text{ K}^{-1}$ . The parameter values are taken from  
691 the multi-model mean of values diagnosed from 16 CMIP5 models  
692 (55). The radiative forcing and temperature anomalies at  $t_0 = 2020$   
693 relative to preindustrial are  $F(t_0) - F(t_{\text{pre}}) = 2.5 \text{ W m}^{-2}$  and  
694  $T_0 \equiv T(t_0) - T(t_{\text{pre}}) = 1.1 \text{ K}$ , where we set  $F_0 \equiv F(t_0) = 0 \text{ W m}^{-2}$   
695 and  $T(t_{\text{pre}}) = 0 \text{ K}$  for convenience.

696 Since, by construction, the anthropogenic forcing  $F(t)$  varies on  
697 timescales longer than the fast relaxation timescale  $\tau_U = C_U/(B +$   
698  $\kappa) = 4$  years, we can ignore the time-dependence in the upper ocean  
699 and approximate

$$T \approx \frac{F + \kappa T_D}{B + \kappa}, \quad [17] \quad 700$$

701 where the evolution of the deep ocean

$$C_D \frac{dT_D}{dt} \approx -\frac{B\kappa}{B + \kappa} T_D + \frac{\kappa}{B + \kappa} F \quad [18] \quad 702$$

703 occurs on a slower timescale  $\tau_D \equiv \frac{C_D}{B} \frac{B + \kappa}{\kappa} = 240 \text{ years}$  (77).  
704 This approximation is convenient because it permits a simple closed  
705 form solution, but should be avoided if the model is applied to  
706 scenarios with rapidly changing forcing, such as studies of the tran-  
707 sient response to an instantaneous doubling of CO<sub>2</sub> or the SRM  
708 "termination effect" (see SI Text 1 for validation of the approxima-  
709 tion). Plugging the exact solution to eq. 18 into eq. 17 gives the  
710 closed-form solution

$$T(t) - T_0 = \frac{F(t)}{B + \kappa} + \frac{\kappa}{B} \frac{1}{(B + \kappa)} \int_{t_0}^t \frac{e^{-(t-t')/\tau_D}}{\tau_D} F(t') dt'. \quad [19] \quad 711$$

706 The evolution of the controlled temperature anomaly (eq. 5; Figure  
707 2c) has the same form but is instead driven by the controlled net  
708 radiative forcing  $F_{M,R,G}$ .

709 We identify the first term on the right hand side of eq. 19 and  
710 eq. 5 as the transient climate response (78), which dominates for  
711  $t - t_0 \ll \tau_D$ , while the second term is a slower “recalcitrant” response  
712 due to a weakening of ocean heat uptake as the deep ocean comes  
713 to equilibrium with the upper ocean (77). While the contribution  
714 of the recalcitrant component to historical warming is thought to  
715 be small, it contributes significantly to 21st century and future  
716 warming (77, 78).

717 The behavior of the model on short and long timescales is illus-  
718 trated by applying it to the canonical climate change experiment in  
719 which  $\text{CO}_2$  concentrations increase at 1% per year until doubling.  
720 The temperature anomaly first rapidly increases until it reaches the  
721 Transient Climate Sensitivity  $TCS = \frac{F_{2\times}}{B + \kappa} = 1.9^\circ\text{C}$  around the  
722 time of doubling  $t = t_{2\times}$ , with  $t_{2\times} - t_0 \ll \tau_D$  and  $F_{2\times} = \alpha \ln(2)$ ,  
723 and then gradually asymptotes to the Equilibrium Climate Sensi-  
724 tivity  $ECS = \frac{F_{2\times}}{B} = 3.1^\circ\text{C} > TCS$  on a much longer timescale  
725  $t - t_0 \gg \tau_D$ .

726 **Model validation.** In Section 1 of the SI, we show that subjecting the  
727 MARGO energy balance model to a stylized RCP8.5-like forcing  
728 accurately reproduces the multi-model mean response from an  
729 ensemble of 35 comprehensive general circulation climate models  
730 from the CMIP5 ensemble (Figure S2). In SI Text 3, we show that  
731 by tweaking just a few of these default parameter values (SI Tables 1  
732 and 2), the model replicates the qualitative results of studies ranging  
733 from analytical control theory analysis of SRM deployments (65)  
734 to numerical optimizations of mitigation, CDR, and SRM deployments  
735 in a recent application of DICE (6), a commonly used Integrated  
736 Assessment Model (26).

737 **ACKNOWLEDGMENTS.** This material is based upon work sup-  
738 ported by the National Science Foundation Graduate Research  
739 Fellowship Program under Grant No. 174530. Any opinions, find-  
740 ings, and conclusions or recommendations expressed in this material  
741 are those of the author(s) and do not necessarily reflect the views  
742 of the National Science Foundation.

743 1. GP Peters, et al., Carbon dioxide emissions continue to grow amidst slowly emerging climate  
744 policies. *Nat. Clim. Chang.* **10**, 3–6 (2020) Number: 1 Publisher: Nature Publishing Group.  
745 2. Intergovernmental Panel on Climate Change, *Global warming of 1.5°C*. (2018) OCLC:  
746 1056192590.  
747 3. EA Parson, Opinion: Climate policymakers and assessments must get serious about climate  
748 engineering. *Proc. Natl. Acad. Sci.* **114**, 9227–9230 (2017) Publisher: National Academy of  
749 Sciences Section: Opinion.  
750 4. JM Deutch, Joint allocation of climate control mechanisms is the cheapest way to reduce  
751 global climate damage. *MIT Cent. for Energy Environ. Policy Res. Work. Pap. Ser.* (2019).  
752 5. J Moreno-Cruz, G Wagner, D Keith, An Economic Anatomy of Optimal Climate Policy. (Social  
753 Science Research Network, Rochester, NY), SSRN Scholarly Paper ID 3001221 (2018).  
754 6. M Belaia, Optimal Climate Strategy with Mitigation, Carbon Removal, and Solar Geoengi-  
755 neering. *arXiv:1903.02043 [econ, q-fin]* (2019) arXiv: 1903.02043.  
756 7. JR Lamontagne, PM Reed, G Marangoni, K Keller, GG Garner, Robust abatement pathways  
757 to tolerable climate futures require immediate global action. *Nat. Clim. Chang.* **9**, 290–294  
758 (2019) Number: 4 Publisher: Nature Publishing Group.  
759 8. EA Parson, DW Keith, End the Deadlock on Governance of Geoengineering Research. *Sci-*  
760 *ence* **339**, 1278–1279 (2013) Publisher: American Association for the Advancement of Sci-  
761 ence Section: Policy Forum.  
762 9. S Schäfer, et al., Field tests of solar climate engineering. *Nat. Clim. Chang.* **3**, 766–766  
763 (2013) Number: 9 Publisher: Nature Publishing Group.  
764 10. K Caldeira, KL Ricke, Prudence on solar climate engineering. *Nat. Clim. Chang.* **3**, 941–941  
765 (2013) Number: 11 Publisher: Nature Publishing Group.  
766 11. W Steffen, et al., Trajectories of the Earth System in the Anthropocene. *Proc. Natl. Acad. Sci.*  
767 *United States Am.* **115**, 8252–8259 (2018).  
768 12. S Manabe, RT Wetherald, Thermal equilibrium of the atmosphere with a given distribution of  
769 relative humidity. *J. Atmospheric Sci.* **24**, 241–259 (1967).  
770 13. R Revelle, W Broecker, H Craig, C Kneeling, J Smagorinsky, Restoring the quality of our  
771 environment: report of the environmental pollution panel. Atmospheric carbon dioxide. *Pres-*  
772 *ident’s Science Advisory Committee, United States, US Government Printing Office: Wash-*  
773 *ington, DC* (1965).  
774 14. WW Kellogg, SH Schneider, Climate Stabilization: For Better or for Worse? *Science* **186**,  
775 1163–1172 (1974) Publisher: American Association for the Advancement of Science Section:  
776 Articles.  
777 15. NR Council, et al., Policy implications of greenhouse warming in *Report of the Committee*  
778 *on Science, Engineering and Public Policy*. (National Academy Press Washington, DC), p.  
779 127 (1991).

780 16. PJ Crutzen, Albedo Enhancement by Stratospheric Sulfur Injections: A Contribution to Re-  
781 solve a Policy Dilemma? *Clim. Chang.* **77**, 211 (2006).  
782 17. DG Victor, MG Morgan, F Apt, J Steinbruner, The Geoengineering Option - A Last Resort  
783 against Global Warming Essay. *Foreign Aff.* **88**, 64–76 (2009).  
784 18. HJ Buck, Geoengineering: Re-making Climate for Profit or Humanitarian Intervention? *Dev.*  
785 *Chang.* **43**, 253–270 (2012) \_eprint: [https://onlinelibrary.wiley.com/doi/pdf/10.1111/j.1467-](https://onlinelibrary.wiley.com/doi/pdf/10.1111/j.1467-7660.2011.01744.x)  
786 [7660.2011.01744.x](https://onlinelibrary.wiley.com/doi/pdf/10.1111/j.1467-7660.2011.01744.x).  
787 19. J McClellan, DW Keith, J Apt, Cost analysis of stratospheric albedo modification delivery  
788 systems. *Environ. Res. Lett.* **7**, 034019 (2012) Publisher: IOP Publishing.  
789 20. K Dow, et al., Limits to adaptation. *Nat. Clim. Chang.* **3**, 305–307 (2013) Number: 4 Publisher:  
790 Nature Publishing Group.  
791 21. JA Flegal, A Gupta, Evoking equity as a rationale for solar geoengineering research? Scruti-  
792 nizing emerging expert visions of equity. *Int. Environ. Agreements: Polit. Law Econ.* **18**,  
793 45–61 (2018).  
794 22. B Haerlin, D Parr, How to restore public trust in science. *Nature* **400**, 499–499 (1999) Number:  
795 6744 Publisher: Nature Publishing Group.  
796 23. J Lacey, M Howden, C Cvitanovic, RM Colvin, Understanding and managing trust at the  
797 climate science–policy interface. *Nat. Clim. Chang.* **8**, 22–28 (2018) Number: 1 Publisher:  
798 Nature Publishing Group.  
799 24. KL Ricke, JB Moreno-Cruz, K Caldeira, Strategic incentives for climate geoengineering coalitions  
800 to exclude broad participation. *Environ. Res. Lett.* **8**, 014021 (2013) Publisher: IOP  
801 Publishing.  
802 25. JA Flegal, AM Hubert, DR Morrow, JB Moreno-Cruz, Solar Geoengineering: Social Science,  
803 Legal, Ethical, and Economic Frameworks. *Annu. Rev. Environ. Resour.* **44**, 399–423 (2019)  
804 \_eprint: <https://doi.org/10.1146/annurev-environ-102017-030032>.  
805 26. WD Nordhaus, An Optimal Transition Path for Controlling Greenhouse Gases. *Science* **258**,  
806 1315–1319 (1992) Publisher: American Association for the Advancement of Science Section:  
807 Articles.  
808 27. G Luderer, et al., Economic mitigation challenges: how further delay closes the door for  
809 achieving climate targets. *Environ. Res. Lett.* **8**, 034033 (2013) Publisher: IOP Publishing.  
810 28. United Nations Framework Convention on Climate Change, Paris agreement. Article 2(a)  
811 (<https://unfccc.int/process-and-meetings/the-paris-agreement/the-paris-agreement>) (2015).  
812 29. J Rogelj, et al., Paris Agreement climate proposals need a boost to keep warming well below  
813 2°C. *Nature* **534**, 631–639 (2016) Number: 7609 Publisher: Nature Publishing Group.  
814 30. J Weyant, Some Contributions of Integrated Assessment Models of Global Climate Change.  
815 *Rev. Environ. Econ. Policy* **11**, 115–137 (2017) Publisher: Oxford Academic.  
816 31. J Bezanson, A Edelman, S Karpinski, V Shah, Julia: A Fresh Approach to Numerical Com-  
817 puting. *SIAM Rev.* **59**, 65–98 (2017).  
818 32. W Nordhaus, P Satorc, Dice 2013r: Introduction and user’s manual. *Yale Univ. Natl. Bureau*  
819 *Econ. Res. USA* (2013).  
820 33. K Riahi, et al., The Shared Socioeconomic Pathways and their energy, land use, and green-  
821 house gas emissions implications: An overview. *Glob. Environ. Chang.* **42**, 153–168 (2017).  
822 34. S Solomon, GK Plattner, R Knutti, P Friedlingstein, Irreversible climate change due to car-  
823 bon dioxide emissions. *Proc. Natl. Acad. Sci.* **106**, 1704–1709 (2009) Publisher: National  
824 Academy of Sciences Section: Physical Sciences.  
825 35. DP Marshall, L Zanna, A Conceptual Model of Ocean Heat Uptake under Climate Change. *J.*  
826 *Clim.* **27**, 8444–8465 (2014) Publisher: American Meteorological Society.  
827 36. S Fuss, et al., Negative emissions—Part 2: Costs, potentials and side effects. *Environ. Res.*  
828 *Lett.* **13**, 063002 (2018) Publisher: IOP Publishing.  
829 37. M Lickley, BB Cael, S Solomon, Time of Steady Climate  
830 Change. *Geophys. Res. Lett.* **46**, 5445–5451 (2019) \_eprint:  
831 <https://agupubs.onlinelibrary.wiley.com/doi/pdf/10.1029/2018GL081704>.  
832 38. HD Matthews, K Caldeira, Stabilizing climate requires near-  
833 zero emissions. *Geophys. Res. Lett.* **35** (2008) \_eprint:  
834 <https://agupubs.onlinelibrary.wiley.com/doi/pdf/10.1029/2007GL032388>.  
835 39. MJ Glotter, RT Pierrehumbert, JW Elliott, NJ Matteson, EJ Moyer, A simple carbon cycle  
836 representation for economic and policy analyses. *Clim. Chang.* **126**, 319–335 (2014).  
837 40. P Christensen, K Gillingham, W Nordhaus, Uncertainty in forecasts of long-run economic  
838 growth. *Proc. Natl. Acad. Sci.* **115**, 5409–5414 (2018).  
839 41. C Azar, SH Schneider, Are the economic costs of stabilising the atmosphere prohibitive?  
840 *Ecol. Econ.* **42**, 73–80 (2002).  
841 42. N Glanemann, SN Willner, A Levermann, Paris Climate Agreement passes the cost-benefit  
842 test. *Nat. Commun.* **11**, 1–11 (2020) Number: 1 Publisher: Nature Publishing Group.  
843 43. FP Ramsey, A Mathematical Theory of Saving. *The Econ. J.* **38**, 543–559 (1928) Publisher:  
844 [Royal Economic Society, Wiley].  
845 44. RM Solow, The Economics of Resources or the Resources of Economics. *The Am. Econ.*  
846 *Rev.* **64**, 1–14 (1974) Publisher: American Economic Association.  
847 45. N Stern, NH Stern, GB Treasury, *The Economics of Climate Change: The Stern Review*.  
848 (Cambridge University Press), (2007).  
849 46. K Arrow, et al., Determining Benefits and Costs for Future Generations. *Science* **341**, 349–  
850 350 (2013) Publisher: American Association for the Advancement of Science Section: Policy  
851 Forum.  
852 47. SH Schneider, The Greenhouse Effect: Science and Policy. *Science* **243**, 771–781 (1989)  
853 Publisher: American Association for the Advancement of Science Section: Articles.  
854 48. RSJ Tol, Is the Uncertainty about Climate Change too Large for Expected Cost-Benefit Anal-  
855 ysis? *Clim. Chang.* **56**, 265–289 (2003).  
856 49. J Koomey, Moving beyond benefit–cost analysis of climate change. *Environ. Res. Lett.* **8**,  
857 041005 (2013) Publisher: IOP Publishing.  
858 50. RB Alley, et al., Abrupt Climate Change. *Science* **299**, 2005–2010 (2003).  
859 51. M Burke, SM Hsiang, E Miguel, Global non-linear effect of temperature on economic produc-  
860 tion. *Nature* **527**, 235–239 (2015) Number: 7577 Publisher: Nature Publishing Group.  
861 52. JK Hammit, Evaluation Endpoints and Climate Policy: Atmospheric Stabilization, Benefit-  
862 Cost Analysis, and Near-Term Greenhouse-Gas Emissions. *Clim. Chang.* **41**, 447–468  
863 (1999).

- 864 53. JP Weyant, A Critique of the Stern Review's Mitigation Cost Analyses and Integrated Assess-  
865 ment. *Rev. Environ. Econ. Policy* **2**, 77–93 (2008) Publisher: Oxford Academic.
- 866 54. R Millar, M Allen, J Rogelj, P Friedlingstein, The cumulative carbon budget and its implications.  
867 *Oxf. Rev. Econ. Policy* **32**, 323–342 (2016) Publisher: Oxford Academic.
- 868 55. O Geoffroy, et al., Transient Climate Response in a Two-Layer Energy-Balance Model. Part  
869 I: Analytical Solution and Parameter Calibration Using CMIP5 AOGCM Experiments. *J. Clim.*  
870 **26**, 1841–1857 (2012) Publisher: American Meteorological Society.
- 871 56. RJ Lempert, ME Schlesinger, SC Bankes, When we don't know the costs or the benefits:  
872 Adaptive strategies for abating climate change. *Clim. Chang.* **33**, 235–274 (1996).
- 873 57. G Wagner, RJ Zeckhauser, Confronting Deep and Persistent Climate Uncertainty, (Social  
874 Science Research Network, Rochester, NY), SSRN Scholarly Paper ID 2818035 (2016).
- 875 58. S Shayegh, VM Thomas, Adaptive stochastic integrated assessment modeling of optimal  
876 greenhouse gas emission reductions. *Clim. Chang.* **128**, 1–15 (2015).
- 877 59. B Crost, CP Traeger, Optimal climate policy: Uncertainty versus Monte Carlo. *Econ. Lett.*  
878 **120**, 552–558 (2013).
- 879 60. M Webster, N Santen, P Parpas, An approximate dynamic programming framework for mod-  
880 eling global climate policy under decision-dependent uncertainty. *Comput. Manag. Sci.* **9**,  
881 339–362 (2012).
- 882 61. JB Moreno-Cruz, Mitigation and the geoengineering threat. *Resour. Energy Econ.* **41**, 248–  
883 263 (2015).
- 884 62. S Fuss, et al., Betting on negative emissions. *Nat. Clim. Chang.* **4**, 850–853 (2014) Number:  
885 10 Publisher: Nature Publishing Group.
- 886 63. RS Tol, On the optimal control of carbon dioxide emissions: an application of FUND. *Environ.*  
887 *Model. & Assess.* **2**, 151–163 (1997).
- 888 64. C Hope, The marginal impact of co2 from page2002: an integrated assessment model incor-  
889 porating the ipcc's five reasons for concern. *Integr. assessment* **6** (2006).
- 890 65. SA Soldatenko, RM Yusupov, Optimal Control of Aerosol Emissions into the Stratosphere to  
891 Stabilize the Earth's Climate. *Izvestiya, Atmospheric Ocean. Phys.* **54**, 480–486 (2018).
- 892 66. SH Schneider, Integrated assessment modeling of global climate change: Transparent ratio-  
893 nal tool for policy making or opaque screen hiding value-laden assumptions? *Environ. Model.*  
894 *& Assess.* **2**, 229–249 (1997).
- 895 67. RS Pindyck, The Use and Misuse of Models for Climate Policy. *Rev. Environ. Econ. Policy*  
896 **11**, 100–114 (2017) Publisher: Oxford Academic.
- 897 68. HJ Buck, What can geoengineering do for us? public participation and the new media land-  
898 scape in *Paper for workshop: The ethics of solar radiation management, 18 Oct 2010, Uni-*  
899 *versity of Montana.* (2010).
- 900 69. LE Clarke, et al., Assessing Transformation Pathways. In: Climate Change 2014: Mitigation  
901 of Climate Change. Contribution of Working Group III to the Fifth Assessment Report of the  
902 Intergovernmental Panel on Climate Change, Technical report (2014).
- 903 70. PJ Irvine, et al., Towards a comprehensive climate impacts assess-  
904 ment of solar geoengineering. *Earth's Futur.* **5**, 93–106 (2017) \_eprint:  
905 <https://agupubs.onlinelibrary.wiley.com/doi/pdf/10.1002/2016EF000389>.
- 906 71. M Goes, N Tuana, K Keller, The economics (or lack thereof) of aerosol geoengineering. *Clim.*  
907 *Chang.* **109**, 719–744 (2011).
- 908 72. A Wächter, LT Biegler, On the implementation of an interior-point filter line-search algorithm  
909 for large-scale nonlinear programming. *Math. Program.* **106**, 25–57 (2006).
- 910 73. LS Siegel, et al., En-roads simulator reference guide, (Technical Report), Technical report  
911 (2018).
- 912 74. M Ha-Duong, MJ Grubb, JC Hourcade, Influence of socioeconomic inertia and uncertainty on  
913 optimal CO<sub>2</sub>-emission abatement. *Nature* **390**, 270–273 (1997) Number: 6657 Publisher:  
914 Nature Publishing Group.
- 915 75. HJ Buck, Rapid scale-up of negative emissions technologies: social barriers and social impli-  
916 cations. *Clim. Chang.* **139**, 155–167 (2016).
- 917 76. JC Minx, et al., Negative emissions—Part 1: Research landscape and synthesis. *Environ.*  
918 *Res. Lett.* **13**, 063001 (2018) Publisher: IOP Publishing.
- 919 77. IM Held, et al., Probing the Fast and Slow Components of Global Warming by Returning  
920 Abruptly to Preindustrial Forcing. *J. Clim.* **23**, 2418–2427 (2010).
- 921 78. JM Gregory, PM Forster, Transient climate response estimated from radiative forcing and  
922 observed temperature change. *J. Geophys. Res. Atmospheres* **113** (2008).

1

## 2 **Supplementary Information for**

### 3 **A multi-control climate policy process for a trusted decision maker**

4 **Henri F. Drake, Ronald L. Rivest, Alan Edelman, and John Deutch**

5 **Corresponding Author: Ronald L. Rivest.**

6 **E-mail: rivest@mit.edu**

#### 7 **This PDF file includes:**

8     Supplementary text

9     Figs. S1 to S5

10    Tables S1 to S2

11    SI References

## 12 Supporting Information Text

13 Figure S1 shows the same information as Figure 2 of the main text, but for the cost-benefit analysis rather than the  
14 cost-effectiveness analysis.

### 15 1. Validation of MARGO’s approximate two-box Energy Balance Model

16 **A. Comparison with CMIP5 simulations under RCP8.5.** The two-box Energy Balance Model (EBM) used in the MARGO  
17 model is described in the main text Methods. Here, we validate the MARGO-EBM by comparing it to an ensemble of 35  
18 CMIP5 models under the RCP8.5 forcing scenario. We further validate the MARGO-EBM’s approximation to the two-layer box  
19 model (in the equilibrated-thermocline limit  $C_U \ll C_D$ ). We validate the approximation in three different high-forcing regimes:  
20 1) the RCP8.5 scenario with large but gradual changes in forcing over the 21st Century; 2) the long-term (800 year) approach  
21 to equilibrium in an extended RCP8.5 scenario (ECP8.5); and 3) the short-term response to deployment and termination of  
22 large-amplitude solar radiation modification (SRM).

23 First, we construct an idealized forcing scenario that is meant to approximate RCP8.5 (1) and its extension beyond 2100,  
24 ECP8.5 (2). In our scenario, baseline  $\text{CO}_{2e}$  emissions: 1) increase exponentially with a growth rate of  $1/37 \text{ years}^{-1}$  to reach a  
25 maximum of  $410 \text{ GtCO}_{2e}/\text{year}$  in 2100, approximately 7 times present-day emissions; 2) plateau between 2100 and 2120; and 3)  
26 decrease linearly to zero between 2120 and 2200 (Figure S2a). As a result,  $\text{CO}_{2e}$  concentrations increase exponentially from  
27 the preindustrial value  $c_0 = 280 \text{ ppm}$  in 1850 to  $1400 \text{ ppm}$  in 2100. In the extended scenario ECP8.5,  $\text{CO}_{2e}$  concentrations  
28 continue to grow until stabilizing at  $3000 \text{ ppm}$  in  $2200^*$  (Figure S2b). These increases in  $\text{CO}_{2e}$  drive a radiative forcing which  
29 increases to  $F = 8.5 \text{ W/m}^2$  by 2100 and stabilizes at  $F = 12 \text{ W/m}^2$  by 2200 (Figure S2c). The forcing timeseries constructed  
30 here approximates the RCP8.5 and ECP8.5 scenarios reasonably well— compare our Figure S2c with Figure 4 of Meinshausen  
31 et al (2011; 2).

32 When subjecting the MARGO-EBM to the RCP8.5-like scenario introduced above, we almost exactly recover the multi-  
33 model-mean warming from the CMIP5 ensemble under RCP8.5 (Figure S2d, solid black and blue lines). The excellent agreement  
34 is not surprising, given that we have tuned our MARGO-EBM with parameter values calibrated to the CMIP5 models (3).  
35 The climate physics-based calibration used here (3) is more realistic than the calibrations of commonly-used IAMs (4) and  
36 more robust to out-of-sample climate forcings.

37 **B. Evaluation of the equilibrated-thermocline approximation.** The MARGO-EBM uses the equilibrated-thermocline approxi-  
38 mation,

$$39 \quad T_{M,R,G}(t) - T_0 = \frac{F_{M,R,G}(t)}{B + \kappa} + \frac{\kappa}{B} \int_{t_0}^t e^{-\frac{t-t'}{\tau_D}} \frac{F_{M,R,G}(t')}{B + \kappa} dt', \quad [1]$$

which is a valid solution of the two-layer equations

$$40 \quad C_U \frac{dT}{dt} = -BT - \kappa(T - T_D) + F(t), \quad [2]$$

$$41 \quad C_D \frac{dT_D}{dt} = \kappa(T - T_D), \quad [3]$$

42 in the limit  $C_U \ll C_D$ . In Figure S2e we show that this approximation (dashed black line) introduces only very small errors  
43 relative to the full solution under the ECP8.5 forcing scenario (solid black line). The full solution is computed numerically by  
44 solving the two-layer EBM equations 2 and 3 using forward finite differences. If we dramatically reduce either the deep ocean  
45 heat uptake rate  $\kappa$  or the deep ocean heat capacity  $C_D$ , as is customary in IAMs (4), then the model 1) equilibrates much too  
46 quickly with the instantaneous forcing and 2) underestimates recalcitrant changes that occurs long after the radiative forcing is  
47 stabilized (Figure S2e, dotted black line).

48 Since we are interested in the response of the MARGO-EBM to climate controls which may cause the controlled radiative  
49 forcing  $F_{M,R,G}$  to deviate substantially from a high-emissions baseline scenario, we here validate the MARGO-EBM’s response  
50 to a short-term impulse of radiative forcing. In Figure S3, we modify the above ECP8.5 scenario by adding a Gaussian negative  
51 radiative forcing anomaly due to short-term SRM. The negative forcing impulse is centered around 2075, has a magnitude of  
52  $F_G = -GF(t \rightarrow \infty) = -3.4 \text{ Wm}^{-2}$  (for  $G = 40\%$ ), and a timescale of  $\sigma = 20 \text{ years}$  (Figure S3a). This negative forcing results  
53 in a pronounced short-term *net cooling* between 2050-2070, followed by an extremely rapid warming from 2070 to 2080 as the  
54 SRM program terminates (Figure S3b,c). A weak residual cooling of  $0.1 \text{ }^\circ\text{C}$  propagates into the deep ocean and lingers for  
55 centuries (Figure S3c). Despite the neglect of upper-ocean thermal inertia in the equilibrated-thermocline approximation, the  
56 MARGO-EBM agrees well with the full solution of the two-box equations, the approximation lagging behind the full solution  
57 by roughly  $\tau_U = 5 \text{ years}$  (Figure S3c).

### 56 2. Comprehensive model equations and parameter values

57 In the cost-effectiveness framing, the full formulation of the problem

$$58 \quad \min \{ \text{discounted costs} \} \quad \text{subject to} \quad T_{M,R,G,A} < T^*$$

\*In the original definition of the ECP8.5 scenario (2), much of these  $\text{CO}_{2e}$  increases are the result of increases in other gases such as Methane, Nitrous Oxide, and Hydrofluorocarbons.

is given, in closed form, by:

$$\min \left\{ [E_0(1 + \gamma)^{(t-t_0)} (\tilde{C}_M M^2 + \tilde{C}_G G^2) + C_R R^2 + C_A A^2] (1 + \rho)^{-(t-t_0)} \right\} \quad [4]$$

Subject to

$$\sqrt{1-A} \left[ T_0 + \frac{a \ln \left( \frac{c_0 + \int_{t_0}^t r q (1-M) dt' - q_0 \int_{t_0}^t R dt'}{c_0} \right) - F_\infty G}{B + \kappa} + \frac{\kappa}{B} \int_{t_0}^t \frac{e^{-\frac{t'-t}{\tau_D}}}{\tau_D} \left\{ \frac{a \ln \left( \frac{c_0 + \int_{t_0}^{t'} r q (1-M) dt'' - q_0 \int_{t_0}^{t'} R dt''}{c_0} \right) - F_\infty G}{B + \kappa} \right\} dt' \right] < T^*, \quad [5]$$

59 where  $\tau_D = \frac{C_D B + \kappa}{B \kappa}$  is a timescale specified by the physical parameter  $C_D$ . The cost-benefit equation can similarly be  
60 derived based on the equations in the main text.

61 The problem is fully characterized by the 19 "free" parameters in equations 4 and 5, the default values of which are reported  
62 in Table S1 (18 in the case of cost-effectiveness, which avoids the use of a poorly-constrained damage coefficient  $\beta$ ). The 19  
63 parameters are: 3 grid parameters  $t_0, t_f, \delta t$ ; the 3 initial conditions  $T_0, c_0, E_0$ ; the 1 carbon cycle parameter  $r$ ; the 4 physical  
64 parameters  $a, B, \kappa$ , and  $C_D$ ; the 3 economic parameters  $\beta, \rho, \gamma$ ; and the 5 control cost parameters  $C_A, C_R, \tilde{C}_M, \tilde{C}_G, F_\infty$ .  
65 The baseline emissions timeseries  $q(t)$  is treated as exogenous and must be prescribed as an input. In the cost-effectiveness  
66 framework, the poorly-constrained damage parameter  $\beta$  is replaced by a prescribed temperature goal  $T^*$ . The grid, initial  
67 condition, and physical parameters are well constrained, while the economic and cost parameters are heuristic interpretations  
68 of the wider climate and economic literature.

69 The control variables  $\alpha \in \mathcal{A} = \{M, R, G, A\}$  satisfy several additional constraints, which could be thought of as an additional  
70 20 parameters, at most, although many end up being unimportant or redundant across several parameters (1 and 2 are necessary  
71 physical constraints on the controls whereas 3, 4, and 5 simply make the model's behavior more realistic):

- 72 1. The controls must be positive,  $\alpha \geq 0$ ;
- 73 2. They have an upper bound:  $\alpha < \alpha_{\max}$ .  $M_{\max} = 1$  is by set by the definition of mitigation.  $G_{\max} = 1$  is chosen because it  
74 results in a negative radiative forcing that exactly offsets the maximum GHG forcing of  $8.5 \text{ W/m}^2$ . We set  $A_{\max} = 40\%$   
75 in acknowledgement of practical (5) and theoretical (6) limits to adaptability (this is meant as more of a symbolic  
76 gesture rather than an estimate of how much climate damage might be adaptable). Finally,  $R = 50\%$  is set based on a  
77 recent bottom-up estimate of the potential for carbon dioxide removal of existing (but not necessarily scalable) negative  
78 emissions technologies.
- 79 3. They have an initial condition  $\alpha(t_0) = \alpha_0$ , which are all set to zero except for  $M_0 = 10\%$ , since none of the other controls  
80 have yet been deployed at scale.
- 81 4. We set maximum deployment and termination rates  $|\frac{d\alpha}{dt}| < \dot{\alpha}$ , which represent economic, technological, and social  
82 inertia. We set  $\dot{M} = \dot{R} = 1/40 \text{ years}^{-1}$  as an upper limit on plausible timescales of global energy transition. On the other  
83 hand, we set  $\dot{G} = 1/20 \text{ years}^{-1}$  to reflect the fact that solar geo-engineering deployment capacity could in principle be  
84 ramped-up very quickly, possibly even in the absence of global governance or regulation. We interpret adaptation costs  
85 as buying insurance against future damages up-front, with both benefits and costs spread evenly in the future. Thus, we  
86 set  $\dot{A} = 0$ . The caveat is that we allow control policy re-evaluations, at which point the value of adaptation can in that  
87 timestep be increased or decreased to a new level (see Figure 5 of main text), without a limit on the rate of increase.
- 88 5. We implement "readiness" constraints,  $\alpha(t) = 0$  for all  $t < t_\alpha$ , to reflect the fact that some controls, such as geoengineering  
89 (both carbon and solar), do not yet exist as climate-relevant socio-technological systems (7). In particular, we set  
90  $t_R = 2030$  and  $t_G = 2050$ .

### 91 3. Qualitative replications of other climate control model analysis

92 To illustrative the potential utility of MARGO as a community tool, we show how run-time parameter values in MARGO can be  
93 tweaked to match the model configurations and results of other studies of climate control policies. One the one hand, MARGO  
94 can be tuned to the inputs and outputs of a comprehensive multi-control IAM configuration to reproduce its qualitative results  
95 (Section A; 8); on the other hand, MARGO can be simplified by setting many of the parameters to zero to emulate an analytical  
96 model of climate control by solar radiation modification (SRM) only (Section B; 9). The goal of this section is to show how  
97 with minimal modifications to the default MARGO model, we are able to replicate key figures from two very different studies.  
98 For discussion of the figures we attempt to replicate, we refer readers to the original studies (8, 9).

Parameter	Default Configuration
$t_0$	2020
$t_f$	2200
$\delta t$	5 yr
$c_0$	460 ppm
$T_0$	1.1 K
$a$	$4.97 \text{ W m}^{-2}$
$r$	50%
$B$	$1.13 \text{ W m}^{-2} \text{ K}^{-1}$
$\kappa$	$0.72 \text{ W m}^{-2} \text{ K}^{-1}$
$C_D$	$106 \text{ W yr m}^{-2} \text{ K}^{-1}$
$\beta$	$0.22 \times 10^{12} \text{ \$ yr}^{-1} \text{ K}^{-2}$
$\rho$	1%
$E_0$	$100 \times 10^{12} \text{ \$ yr}^{-1}$
$\gamma$	2%
$C_A$	$4.5 \times 10^{12} \text{ \$ yr}^{-1}$
$C_R$	$13 \times 10^{12} \text{ \$ yr}^{-1}$
$C_M$	2% (of GWP)
$C_G$	4.6% (of GWP)
$F_\infty$	$8.5 \text{ W m}^{-2}$

**Table S1. Values of the 19 free parameters that characterize the MARGO model.**

99 **A. Belaia (2019): A multi-control extension of DICE with Mitigation, Carbon Dioxide Removal, and Solar Geo-engineering.**  
100 Belaia (2019) extend DICE, a commonly-used globally-aggregated general equilibrium IAM, to include carbon dioxide removal  
101 (CDR) and solar radiative modification– which they refer to as solar geoengineering (SG)– to supplement DICE’s emissions  
102 mitigation in controlling climate damages (8).

103 To implement CDR and SRM, Belaia (2019) make two fundamental changes to DICE. Their modelling of SRM forcing  
104 is identical to ours. In terms of costs, they similarly make the conservative assumption that SRM costs are dominated by  
105 unintended side effects and scale with the damage of an equivalent amount of GHG forcing, but they include this damage cost  
106 as an additive term to the climate damages rather than the control costs. Their approach is thus similar to ours in the case of  
107 cost-benefit analysis, but in the cost-effectiveness case they effectively ignore indirect SRM damages while reaping the benefits  
108 of its low direct costs. The version of DICE they use already permits moderate negative emissions, as an extension of the  
109 emissions mitigation curve to 120%, i.e. 100% mitigation of baseline emissions mitigation plus removal of an addition 20%  
110 of baseline emissions). To extend this further, Belaia (2019) allow for substantial CDR by extending the mitigation curve  
111 indefinitely, although the cost curves are convex such that CDR becomes increasingly expensive. They also appear to have  
112 modified the functional form of emissions mitigation to keep CDR costs relatively low. The rationale for modelling CDR as an  
113 extension of mitigation is unclear, since 1) emissions mitigation and carbon dioxide removal are distinct physical, industrial,  
114 and economic processes and 2) marginal CDR costs today are already lower than the backstop mitigation costs assumed in  
115 their scenarios.

116 To approximate the DICE configuration used by Belaia (2019), we make the changes to MARGO’s default parameter  
117 values reported in Table S2. Notably, we extended the time from 2200 to 2500, increased the reference costs for mitigation by  
118 about 75%, and increased the reference costs for SRM by about 175%. We found it necessary to modify the physical climate  
119 parameters in order to match their  $\text{CO}_{2e}$  concentrations, radiative forcing, and temperatures based on their baseline emissions  
120 scenario  $q(t)$ , which we approximated with piece-wise quadratic functions (Figure S4a, blue line). Additionally, we omit  
121 adaptation and carbon dioxide removal,  $A_{\max} \equiv R_{\max} \equiv 0$ ; we effectively remove the upper limit on mitigation  $M_{\max} = 10$ ; we  
122 increase socio-technological inertia for all controls to  $\dot{\alpha} = 1/90 \text{ years}^{-1}$ ; we set initial mitigation to  $M_0 = 3\%$ ; and we remove  
123 all "readiness" constraints,  $t_\alpha = 2020$ . Additionally, in order to match the mitigation cost curves in their Figure 1 S4, we found  
124 it necessary to decrease the mitigation cost exponent from 2 to 1.8, as compared to 2.8 in DICE-2013 (10) or 2.6 in DICE-2016  
125 (11).

126 Figure S4 shows the results of cost-benefit analysis for: a baseline scenario, a mitigation only scenario, a mitigation and CDR  
127 scenario, and a scenario with mitigation, CDR, and SRM. Figure S4 has been formatted exactly as Figure 4 of Belaia (2019; 8),  
128 which presents the results from equivalent simulations in their extension of DICE, for convenient side-by-side comparison.

129 **B. Soldatenko and Yusupov (2018): Analytical control theory applied to solar radiation modification.** Soldatenko and Yusupov  
130 (2018; 9) develop an analytical model for the optimally cost-effective time-dependent deployment of solar radiation modification  
131 (SRM) which keeps temperatures in all years below  $T^* = T_0 + 1 \text{ }^\circ\text{C}$  and keeps temperatures at their end date of 2100 below  $T_0$ .  
132 Although their representation of SRM forcing is more involved than ours and depends on the mass of sulfate aerosol injected,  
133 the resulting optimization problem is remarkably similar to an SRM-only configuration of the default MARGO model.

134 To approximate Soldatenko and Yusupov (2018)’s analytical model (9), we make the changes to MARGO’s default parameter  
135 values reported in Table S2. Additionally, we omit adaptation, carbon dioxide removal, and mitigation,  $A_{\max} \equiv R_{\max} \equiv$

Parameter	Belaia (2019)	Soldatenko and Yusupov (2018)
$t_0$		
$t_f$	2500	2100
$\delta t$	1 year	1 year
$c_0$		
$T_0$		
$a$		
$r$	75%	
$B$	$0.8 \times 1.13 \text{ W m}^{-2} \text{ K}^{-1}$	
$\kappa$	$0.75 \times 0.72 \text{ W m}^{-2} \text{ K}^{-1}$	
$C_D$	$0.75 \times 106 \text{ W yr m}^{-2} \text{ K}^{-1}$	
$\beta$		
$\rho$	1.5%	
$E_0$		
$\gamma$		
$C_A$		
$C_R$		
$\tilde{C}_M$	3.6% (of GWP)	
$\tilde{C}_G$	12.5% (of GWP)	
$F_\infty$	$7.5 \text{ Wm}^{-2}$	

**Table S2. Values of the 19 free parameters that characterize the MARGO model, modified to replicate results from other models. Blank cells denote parameters that are not changed from the default values in Table S1.**

136  $M_{\max} \equiv 0$ ; we remove all "readiness" constraints,  $t_\alpha = 2020$ , we set  $T^* = 2.1 \text{ }^\circ\text{C}$  ( $1 \text{ }^\circ\text{C}$  above  $T_0$ ) and add an additional constraint  
137  $T_{M,R,G} < T_0$  on the final timestep at  $t_f = 2100$  (the latter is the only modification that required modifying compiled model  
138 source code).

139 Figure S5 shows the result of cost-effectiveness optimization for an SRM-only scenario, which is formatted to be directly  
140 comparable to Figure 3 of (9).

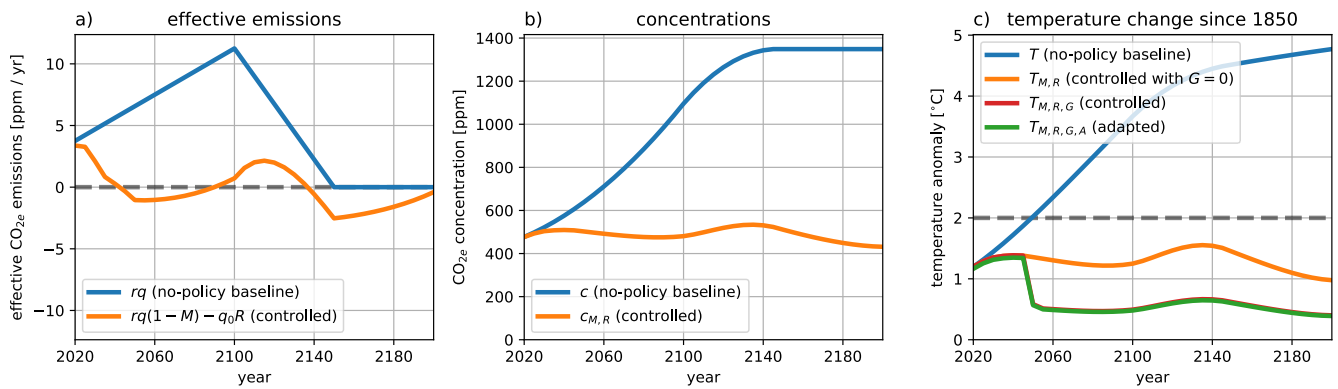


**Fig. S1.** Baseline (blue) and optimally-controlled (orange) a) effective CO<sub>2e</sub> emissions, b) CO<sub>2e</sub> concentrations, and c) temperature anomaly relative to preindustrial from cost-benefit analysis. Panel c) shows the optimal temperature change that would occur: in a baseline scenario (blue); with just emissions **Mitigation** and carbon dioxide **Removal** (orange); with **Mitigation**, **Removal**, and solar-**Geoengineering** (red); and as an “adapted temperature” with **Adaptation** measures also taken into account. The dashed grey line marks 2 °C for context. In (c),  $T_{M,R,G}$  and  $T_{M,R,G,A}$  decrease dramatically in 2050 relative to  $T_{M,R}$  as moderate levels of SRM become permissible.

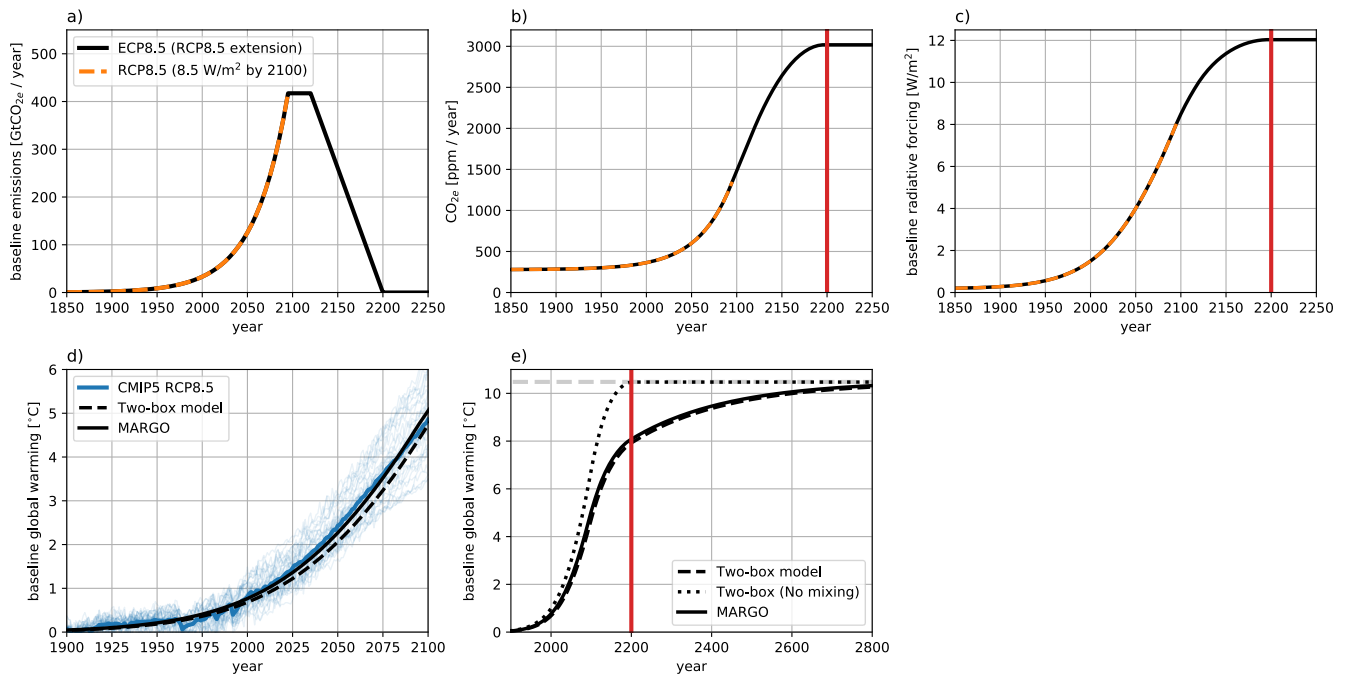


**Fig. S2.** Validation of the 21st Century and equilibrium responses of the MARGO Energy Balance Model (EBM). a) Baseline  $\text{CO}_{2e}$  emissions, b) concentrations, and c) radiative forcing in an RCP8.5-like scenario (dashed orange line) and its extension beyond 2100 (ECP8.5; solid black line). d) The temperature response of CMIP5 models to the RCP8.5 forcing scenario (thin blue lines for individual models; thick blue line for multi-model mean) and of the MARGO-EBM to the RCP8.5-like scenario. The dashed black line shows the full solution to the two-layer equations 2 and 3 with the same parameter values (Geoffroy 2013; 3) as the approximate solution 1 used in the MARGO-EBM. e) The temperature response to the ECP8.5 scenario for: the MARGO-EBM (solid), the full two-box model (dashed black line) and the full two-box model with  $\kappa = 0$  (dotted line). The vertical red lines delineate 2200, the year in which the ECP8.5 emissions reach net zero and concentrations are stabilized.

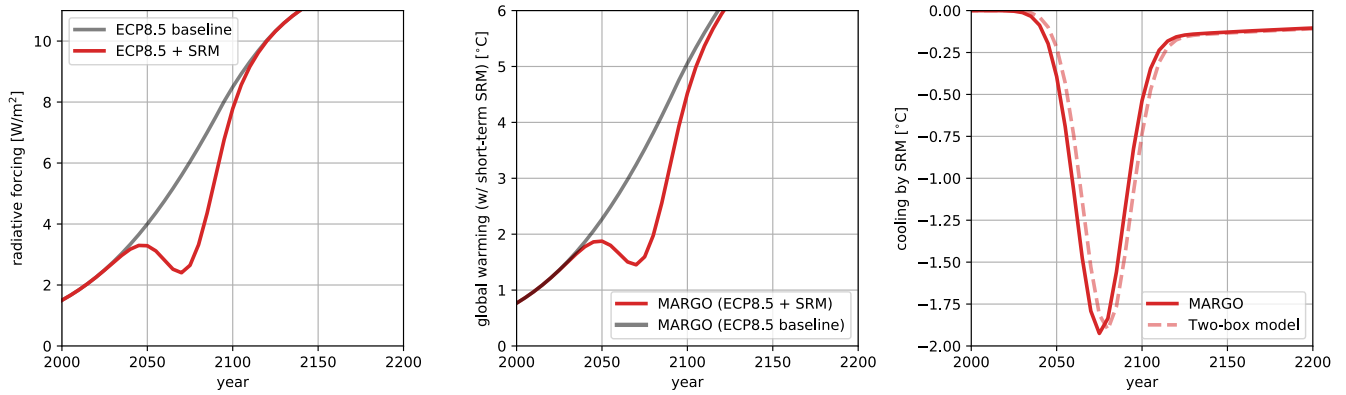


**Fig. S3.** Response of the MARGO-EBM to the ECP8.5 scenario (grey) and to an additional short-term variation in forcing caused by a Gaussian deployment of SRM (red). a) Radiative forcing; b) Temperature response; c) Anomalous cooling in SRM scenario relative to the ECP8.5 baseline in MARGO (solid line) and the full solution to the two-box model (dashed line).

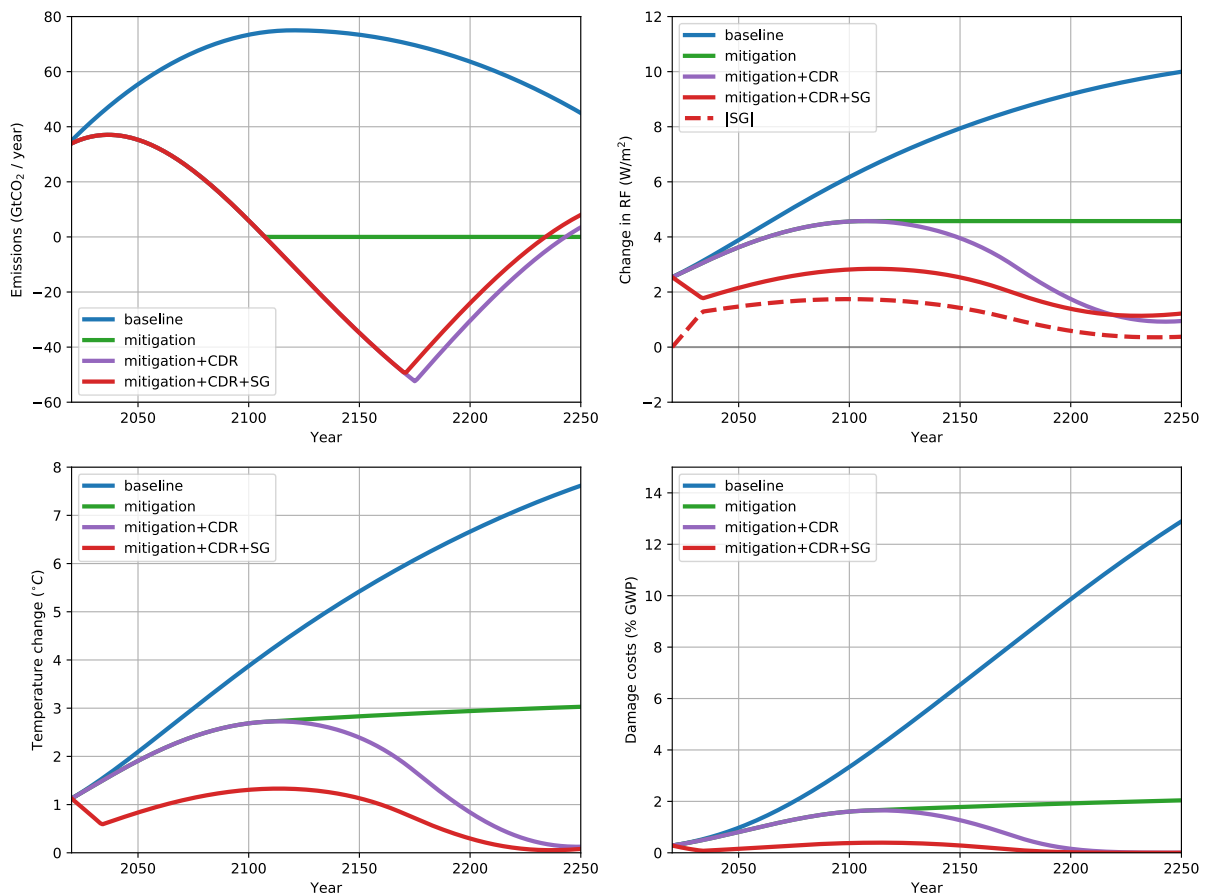
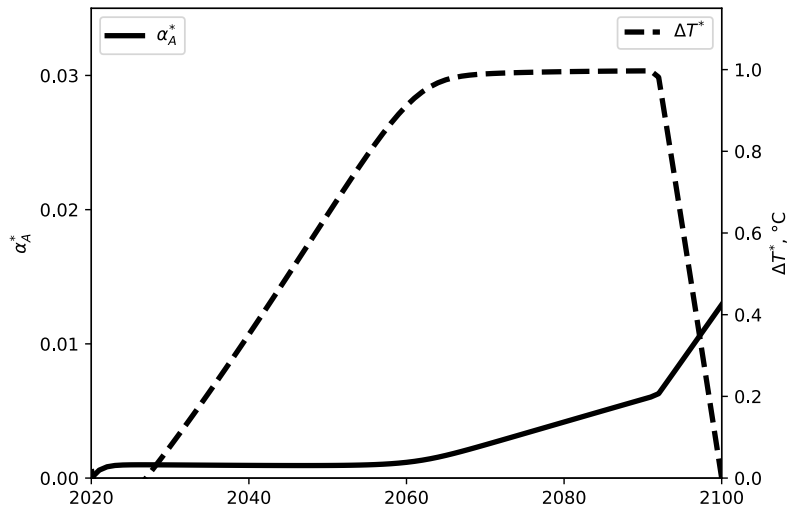


Fig. S4. A qualitative replication of Figure 4 of Belaia (2019; 8); see their figure caption and accompanying discussion of the results.



**Fig. S5.** A qualitative replication of Figure 3 of Soldatenko and Yusupov (2018; 9), who consider the optimally cost-effective deployments of SRM which satisfy the following temperature constraints:  $\Delta T^*(t) \leq 1^{\circ}\text{C}$  and  $\Delta T^*(t_f) \leq 0^{\circ}\text{C}$ , where  $\Delta T^* \equiv T_{M,R,G} - T_0$  is the temperature anomaly relative to 2020 (ignoring mitigation and CDR,  $M \equiv R \equiv 0$ ) and  $t_f = 2100$  is the final date. The dashed curve shows the optimal SRM albedo  $\alpha_A^* \equiv \frac{G(t)F_{\infty}}{S_0/4}$  and the solid black line shows the temperature anomaly  $\Delta T^*$ .

141 **References**

- 142 1. K Riahi, A Grübler, N Nakicenovic, Scenarios of long-term socio-economic and environmental development under climate  
143 stabilization. *Technol. Forecast. Soc. Chang.* **74**, 887–935 (2007).
- 144 2. M Meinshausen, et al., The RCP greenhouse gas concentrations and their extensions from 1765 to 2300. *Clim. Chang.*  
145 **109**, 213 (2011).
- 146 3. O Geoffroy, et al., Transient Climate Response in a Two-Layer Energy-Balance Model. Part I: Analytical Solution  
147 and Parameter Calibration Using CMIP5 AOGCM Experiments. *J. Clim.* **26**, 1841–1857 (2012) Publisher: American  
148 Meteorological Society.
- 149 4. R Calel, DA Stainforth, On the Physics of Three Integrated Assessment Models. *Bull. Am. Meteorol. Soc.* **98**, 1199–1216  
150 (2016) Publisher: American Meteorological Society.
- 151 5. K Dow, et al., Limits to adaptation. *Nat. Clim. Chang.* **3**, 305–307 (2013) Number: 4 Publisher: Nature Publishing Group.
- 152 6. SC Sherwood, M Huber, An adaptability limit to climate change due to heat stress. *Proc. Natl. Acad. Sci.* **107**, 9552–9555  
153 (2010) Publisher: National Academy of Sciences \_eprint: <https://www.pnas.org/content/107/21/9552.full.pdf>.
- 154 7. JA Flegal, AM Hubert, DR Morrow, JB Moreno-Cruz, Solar Geoengineering: Social Science, Legal, Ethical, and Economic  
155 Frameworks. *Annu. Rev. Environ. Resour.* **44**, 399–423 (2019) \_eprint: <https://doi.org/10.1146/annurev-environ-102017-030032>.
- 156 8. M Belaia, Optimal Climate Strategy with Mitigation, Carbon Removal, and Solar Geoengineering. *arXiv:1903.02043*  
157 [*econ, q-fin*] (2019) arXiv: 1903.02043.
- 158 9. SA Soldatenko, RM Yusupov, Optimal Control of Aerosol Emissions into the Stratosphere to Stabilize the Earth’s Climate.  
159 *Izvestiya, Atmospheric Ocean. Phys.* **54**, 480–486 (2018).
- 160 10. W Nordhaus, P Sztorc, Dice 2013r: Introduction and user’s manual. *Yale Univ. Natl. Bureau Econ. Res. USA* (2013).
- 161 11. WD Nordhaus, Revisiting the social cost of carbon. *Proc. Natl. Acad. Sci.* **114**, 1518–1523 (2017) Publisher: National  
162 Academy of Sciences Section: Social Sciences.  
163